Topology of the configuration of eigenvectors and eigenvalues of parametrized Hamiltonians

Zhou Fang*

Abstract

In this article we discuss the topological classification of configuration of eigen vectors and eigenvalues of 2-band and 3-band Hermitian and pseudo Hermitian Hamiltonian.

Contents

*Email: 12333069@mail.sustech.edu.cn

1 Introduction

Topological singularities, arising from points with degenerate eigenvalues in a parametrized Hamiltonian H, are fundamental to many areas of modern physics. These singular points, which include well-known examples such as Weyl and Dirac points and nodal lines, are associated with rich physical phenomena, including topological edge modes and chiral Landau levels. These physical systems can be probed and classified by considering loops in the moduli space of the Hamiltonian, an approach rooted in algebraic topology. The classification of these loops provides insight into the behavior and evolution of eigenvalues and eigenvectors, offering a deeper understanding of the underlying physical systems.

This research seeks to apply algebraic topology, particularly computable invariants, to classify these topological singularities. By focusing on the algebraic and geometric aspects of the problem, we aim to develop a comprehensive framework for understanding the role of topological singularities in various physical contexts.

In Section 2, we first introduce the pioneering work by Mermin. His work motivates many of our ideas. In Section 3, we formulate our problem: classify the topology of configuration of eigenvalues and eigenspaces. In Section 4, we detail discuss three topological invariants using three different methods and compare them in Section 4.4. In Section 5, we provide two methods to classify the 3-band Hermitian Hamiltonian. Both methods are the generalization of methods in Section 4. Then comes the pseudo-Hermitian case. Section 6 uses symmetry of the eigen polynomials to recover the results in [12]. We discuss the generalization of this method in Section 7. Then we use intersection homology to extract topological information of the parameter space of the parametrized matrix in Section 8.

2 Backgrounds

The literature on topological singularities is extensive, with significant contributions across multiple domains. In this section, we briefly review the theory of topological defects established by Mermin in [13], whose pioneering work laid the foundation for this field of research.

Definition 2.1. Let $\mathcal{S}$ be the space of the state at a point, the element in $\mathcal{S}$ is called *order parameter* and $\mathcal{S}$ is called *ordered parameter space*. An *ordered medium* can be described by a map $f : \mathcal{M} \to \mathcal{S}$, where $\mathcal{M}$ is a space.

Example 2.2. (**Planar spins**) Take $\mathcal{M}$ be a region in $\mathbb{R}^3$. Take $\mathcal{S}$ be S^1, a circle. Let $f : \mathcal{M} \to S^1$ defined as $f(\mathbf{r}) = e^{i\phi(\mathbf{r})}$ where $\phi : \mathbb{R}^3 \to [0, 2\pi)$.

This means we assign each point in the $\mathcal{M}$ a unit vector in a plane.

Example 2.3. (**Ordinary spins**) Take $\mathcal{M}$ be a region in $\mathbb{R}^3$. Take $\mathcal{S} = S^2$, a 2-dimension sphere. Let $f : \mathcal{M} \to S^2$ defined as $f(\mathbf{r}) = (u_x(\mathbf{r}), u_y(\mathbf{r}), u_z(\mathbf{r}))$ where u_x, u_y, u_z are three real functions over $\mathcal{M}$ satisfying $u_x^2 + u_y^2 + u_z^2$.

This means we assign each point a 3-dimensional unit vector.

Example 2.4. (**Nematic liquid crystals**) Take $\mathcal{M}$ be a region in $\mathbb{R}^3$. Take $\mathcal{S} = \{\text{lines through origin in } \mathbb{R}^3\} =: \mathbb{RP}^2$, the projection space. Let $f : \mathcal{M} \to \mathbb{RP}^2$ defined as the composition of the maps

$$\mathcal{M} \to \mathbb{R}^3 \to M_{3\times 3}(\mathbb{R})$$

$$\mathbf{r} \mapsto \hat{n}(\mathbf{r}) \mapsto \hat{n}(\mathbf{r})\hat{n}(\mathbf{r})^T$$

The second map is a two to one map, since $\pm\hat{n}$ maps to the same order parameter in $\mathcal{S}$.

This means we assign each point in $\mathcal{M}$ a line (or headless vector).

Example 2.5. (**Biaxial nematics**) Take $\mathcal{M}$ be a region in $\mathbb{R}^3$. Take $\mathcal{S} = \{\text{rectangular box with fixed size centered at oringin in } \mathbb{R}^3\}$.

$\mathcal{S} = SO(3)/D_2$, so an order medium meets above requirements is a space $\mathcal{M}$ with a map $f : \mathcal{M} \to \mathcal{S}$.

Example 2.6. (**Dipole-locked A phase of superfluid helium-3**) Take $\mathcal{M}$ be a region in $\mathbb{R}^3$. Take $\mathcal{S} = \{\text{distinguished orthonormal axes}\}$. Since distinguished orthonormal axes can be viewed as two orthonormal sticks, $\mathcal{S} = SO(3)$.

Next we consider the special case of Brillouin zone BZ. Let $H : BZ \to \mathcal{S}$ be a map assigning each $k \in BZ$ to a Hamiltonian. Let $\iota : S^p \to BZ$ be a null homotopic embedding. So $[H \circ \iota] \in \pi_p(\mathcal{S})$. If $\iota(S^p)$ enclose a node in space $\mathcal{S}$, $\iota(S^p)$ cannot contract to a point and thus $[H \circ \iota] \neq 0$.

Definition 2.7. We call $[H \circ \iota] \in \pi_p(\mathcal{S})$ be a topological charge of the node.

Example 2.8. (**Planar spins**) $\pi_1(S_1) = \mathbb{Z}$, by winding number.

Example 2.9. (**Ordinary spins**) Take $\mathcal{M}$ be a region in $\mathbb{R}^3$. Take $\mathcal{S} = S^2$.

Since all loops on S^2 can be shrink to a constant loop, we have $\pi_1(S^2) = 0$.

Example 2.10. (**Nematic liquid crystals**) $\pi_1(\mathbb{RP}^2) = \pi_1(S^2/\mathbb{Z}_2) = \mathbb{Z}_2$

To figure out the case in biaxial nematics, we need the following useful fact. A detailed proof can be seen in [18].

Fact 2.11. G is a path-connected and simply connected Lie goup and H is a normal group of G. Then

$$\pi_1(G/H) = \pi_0(H) = H/H^0$$

$$\pi_2(G/H) = \pi_1(H^0)$$

where H^0 is the connected component containing identity.

Example 2.12. (**Biaxial nematics**) $\pi_1(SO(3)/D_2) = \pi_1(\cong SU(2)/\overline{D_2}) = \pi_0(\overline{D_2}) = \pi_0 Q = Q$.

$$\pi_2(SO(3)/D_2) = \pi_1(Q^0) = 0$$

Example 2.13. (**Dipole-locked A phase of superfluid helium-3**) $\pi_1(SO(3)) = \pi_1(\mathbb{RP}_3) = \pi_1(S^4/\mathbb{Z}_2) = \mathbb{Z}_2$

When the space is not based, we consider the free homotopy equivalence between maps and then the homotopy group is classified by free homotopy.

Theorem 2.14. Let X be a space. Let f based at x, g based at y be two representation elements of $\pi_1(X)$. Then $f \simeq g$ by free homotopy if and only if there exists a path isomorphism c taking $[f] \in \pi_1(X, x)$ to $[g] \in \pi_1(X, y)$.

This theorem suggests that: Two loops in ordered parameter space are freely homotopic if and only if they are characterized by the same conjugacy class of the fundamental group. Since fusion of nodes corresponds to charge multiplication, it is determined by multiplication rule of conjugacy class.

Example 2.15. (**Multiplication table for quaternian group Q**) The quaternian group Q has following conjugate class: $C_0 := \{1\}$, $\overline{C_0} := -1$, $C_x := \{\pm i\sigma_x\}$, $C_y := \{\pm i\sigma_y\}$, $C_z := \{\pm i\sigma_z\}$. The multiplication table [13] are as following:

$\times$	C_0	$\overline{C_0}$	C_x	C_y	C_z
C_0	C_0	$\overline{C_0}$	C_x	C_y	C_z
$\overline{C_0}$	$\overline{C_0}$	C_0	C_x	C_y	C_z
C_x	C_x	C_x	$2C_0 + 2\overline{C_0}$	$2C_z$	$2C_y$
C_y	C_y	C_y	$2C_z$	$2C_0 + 2\overline{C_0}$	$2C_x$
C_z	C_z	C_z	$2C_y$	$2C_x$	$2C_0 + 2\overline{C_0}$

From the table, we observe that most results in the table consists of unique conjugate group except for some cases where the result is an addition of two conjugate class. That means the result is not unique when we do mutiplication.

Note that the multiplication of two defects is a path connecting two defects and let two defects fusion to another defect along this path. The non unique result is rooted in the non unique way of this path passing through other defects.

Example 2.16. Since $-(i\sigma_x) = (i\sigma_y)(i\sigma_x)(i\sigma_y)^{-1}$, the x defect can converted to its antidefect by passing through y defects. Hence there are two ways to multiplicate two x defects to obtain different results: the first is trivially multiplicate two x defects, we obtain a nontrivial defect; the second is multiplicate two x defects by passing through y defects, we obtain a trivial defect.

We stop introduction to Mermin's study here. Mermin's work introduce homotopy theory into the classification of nodes in band, and later more and more topological tools are applied in this problem, for example, [18], [16], [8],[9],[10],[11].

Mermin's work is studying the topology of ordered medium. In this article, we'll focus on the topology of the configuration of eigenvectors and eigenvalues of parametrized Hamiltonians.

3 Topology of energy bands

The topology of energy bands is the topology of the configuration of eigenvalues and eigenspaces.

Example 3.1. Consider the matrix $H = \begin{bmatrix} f_3 & f_2 \\ -f_2 & -f_3 \end{bmatrix}$, $f_3,\ f_2 \in \mathbb{R}$. We devided the $f_3 - f_2$ plane into three regions: Let $X_0 := \{(0,0)\}$, $X_1 := \{(f_3, f_3), (f_3, -f_3) | f_3 \in \mathbb{R}\}$, $X_2 := \mathbb{R}^2$. Let $\lambda_\pm$ be two eigenvalues and $E(\lambda)$ be the eigenspace.

- X_0: $\lambda_+ = \lambda_- = \lambda$, $dim(E(\lambda)) = 2$
- $X_1 - X_0$: $\lambda_+ = \lambda_- = \lambda$, $dim(E(\lambda)) = 1$
- $X_2 - X_1$: $\lambda_+ \neq \lambda_-$, $dim(E(\lambda_\pm)) = 1$

It's a stratified space with each stratum characterizing different behavior of eigenvalues and eigenvectors.

Definition 3.2. If a point in parametrize space dose not have n distinct eigenvalues, we say it is a singular point.

Example 3.3. (**The swallowtail**)

Consider the parametrized matrix $H = \begin{bmatrix} -f_1 - f_2 + 1 & -f_1 & -f_2 \\ f_1 & f_1 + f_3 & -f_3 \\ f_2 & -f_3 & f_2 + f_3 \end{bmatrix}$, $f_1,\ f_2,\ f_3 \in \mathbb{R}$.

The singular points locally look like a swallowtail [8], see Fig1.

The swallowtail has four singular lines and one of them is an isolated singular line; there is one singular point (meeting point) at the origin. Similarly as previous example, the swallowtail is also a stratified space, see [8].

4 2-band Hermitian Hamiltonians over $\mathbb{R}$

In this section we only consider Hermitian Hamiltonian over $\mathbb{R}$. 2-band Hermitian Hamiltonian over $\mathbb{R}$ is the most simple examples which is also significant. The following ways we only consider loops in gapped region to detect singular points. In this section we provide several ways of classifying singular points by considering loops not intersecting with singular points.

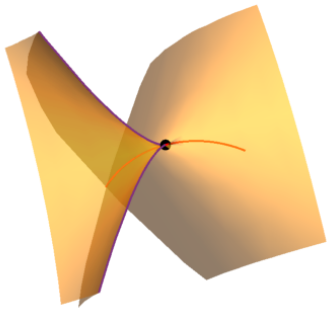

Figure 1: The swallowtail space

4.1 Classifying I: Hopf bundles over $\mathbb{R}$

This section will first review discussion in Section 5.1 in [15], and then apply it to our problem.

Let $Prin_G(S^n)$ be a collection of all principal G-bundles over S^n. Since $Prin_G(S^n) \simeq \pi_{n-1}(G)$, we have $Prin_{S^0}(S^1) \simeq \pi_0(S^0) = \{\pm 1\}$. So there are only two principal S^0-bundles over S^1 (up to isomorphism). More precisely, the two principal S^0-bundles over S^1 are

- trivial bundle: $S^0 \to S^1 \times S^0 \to S^1$ (total space is disconnected)
- Hopf bundle: $S^0 \to S^1 \xrightarrow{h} S^1$ (total space is connected), where $h : S^1 \to S^1, \quad (x_1, x_2) \mapsto (2x_1x_2, x_1^2 - x_2^2)$.

Hence, show that a principal S^0-bundle over S^1 a Hopf bundle is equivalent to show that the total space is connected.

Property 4.1 (Property 4.2 in [15])**.** If we have:
(a) M is a smooth manifold
(b) $H(p)$ is a complex Hermitian $n \times n$ matrix depending smoothly on the parameter $p \in M$
(c) U is an open subset of M fulfilling eigenspace of k-th eigenvalue is one dimensional
Then one can define a principal $U(1)$-bundle (or an S^0-bundle) consisting of normalised of eigenvectors to the k-th eigenvalue of $H(p)$ for all $p \in U$. □

Remark 4.2. Let ψ be a physical state, then ψ and $\lambda\psi$ $\forall \lambda \in U(1)$ corresponding to the same state. This physical meaning motivates the existence of $U(1)$-bundle in above theorem.

Every symmetric real 2×2 matrices can be written as

$$A(a,b,c) = \begin{bmatrix} a+c & b \\ b & a-c \end{bmatrix}, \text{ which has eigenvalues } \lambda_\pm = a \pm \sqrt{c^2+b^2}$$

Consider the eigenbundle corresponding to eigenvalue λ_+.

There is no global representation of normalized eigenvector of λ_+, so we define two open sets: let $U_1 := \mathbb{R}^2 - \{(0,c)|c \leqslant 0\}$ and $U_2 := \mathbb{R}^2 - \{(0,c)|c \geqslant 0\}$.

In U_1, the normalized eigenvector of λ_+ is

$$v_1(a,b,c) = \frac{1}{\sqrt{2(b^2+c^2)+2c\sqrt{c^2+b^2}}} \begin{pmatrix} c+\sqrt{b^2+c^2} \\ b \end{pmatrix}$$

and in U_2, the normalized eigenvector corresponding to λ_+ is

$$v_2(a,b,c) = \frac{1}{\sqrt{2(b^2+c^2)-2c\sqrt{c^2+b^2}}} \begin{pmatrix} b \\ -c+\sqrt{b^2+c^2} \end{pmatrix}$$

Observation: $v_i(a,b,c)$ is independent of a and only depends on b/c, $i = 1,2$.

Example 4.3. On the line $b = 2c$, we have

$$\phi_- = \begin{bmatrix} \frac{1-\sqrt{5}}{2} \\ 1 \end{bmatrix}, \phi_+ = \begin{bmatrix} \frac{1+\sqrt{5}}{2} \\ 1 \end{bmatrix}, c > 0$$

$$\phi_- = \begin{bmatrix} \frac{1+\sqrt{5}}{2} \\ 1 \end{bmatrix}, \phi_+ = \begin{bmatrix} \frac{1-\sqrt{5}}{2} \\ 1 \end{bmatrix}, c < 0$$

□

Therefore, there is a change of base space:

The base space $\mathbb{R}^3 - 0 \xrightarrow{\text{can change to}} \mathbb{R} \times \mathbb{R}_{>0} \times S^1$, see Fig2

The "coordinate" a and r is redundancy, so the eigenbundle is of the form:

$$\pi_0 : \mathbb{R} \times \mathbb{R}_{>0} \times E \to \mathbb{R} \times \mathbb{R}_{>0} \times S^1, \quad (a,r,x) \mapsto (a,r,\pi(x))$$

Where $\pi : E \to S^1$ is a S^0-bundle over S^1. In the following, we only focus on S^0-bundle $\pi : E \to S^1$.

Property 4.4. v_1 defines a local section of E over S^1.

Proof. We want to show $\pi v_1|_{S^1} = id$, i.e., $\pi v_1(x) = x$, $\forall x \in S^1$. It suffices to show $v_1(x) \in \pi^{-1}(x)$. Since $\pi^{-1}(x)$ is the fiber, and $v_1(x)$ is the first eigenvector at x, we have $v_1(x) \in \pi^{-1}(x)$ by construction of eigenbundle. □

$\mathbb{R}^3 \longrightarrow \mathbb{R} \times \mathbb{R} \times S^1$
$(a, b, c) \mapsto (a, r, x)$

a :same a in (a, b, c)
r :strech $r > 0$ times
x :a point x in S^1

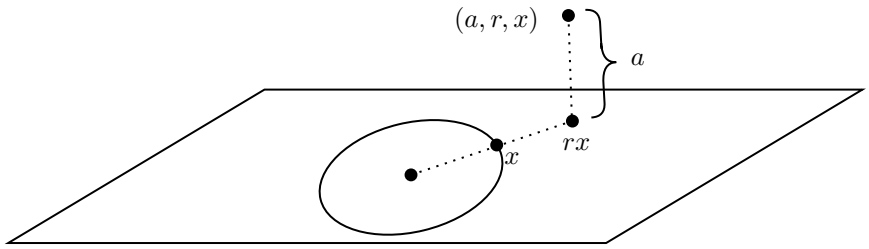

Figure 2: Change base space

Recall that $v_i(a, b, c) = v_j(a, b, c)t_{ji}(a, b, c)$, $i, j = 1, 2$, where t_{12} and t_{21} are transition functions defined on $U_1 \cap U_2 = \mathbb{R}^2 - \{(0, c)|c \in \mathbb{R}\}$. Since eigenvectors only depends on b/c, it suffices to consider them on the circle $b^2 + c^2 = 1$.

$$v_1(a, b, c) = \frac{1}{\sqrt{(c+1)^2 + b^2}} \begin{bmatrix} c+1 \\ b \end{bmatrix} = \frac{1}{\sqrt{b^2(c+1)^2 + b^4}} \begin{bmatrix} |b|\,(c+1) \\ b^2 \end{bmatrix}$$

$$v_2(a, b, c) = \frac{1}{\sqrt{(-c+1)^2 + b^2}} \begin{bmatrix} b \\ -c+1 \end{bmatrix} = \frac{1}{\sqrt{b^2\,(c+1)^2 + (1-c^2)^2}} \begin{bmatrix} b\,(c+1) \\ 1-c^2 \end{bmatrix}$$

$$= \frac{1}{\sqrt{b^2\,(c+1)^2 + b^4}} \begin{bmatrix} b(c+1) \\ b^2 \end{bmatrix}$$

Hence,

$$\text{When } b > 0, \quad t_{12}(b, c) = t_{21}(b, c) = 1$$
$$\text{When } b < 0, \quad t_{12}(b, c) = t_{21}(b, c) = -1$$

Property 4.5. The total space is connected, and thus the bundle is isomorphic to the Hopf bundle.

Proof. By Property 2.23 in [19]: If $\mathcal{U}$ is a connected covering of a topological space X and X has a subset A with $A \cup U_i \neq \emptyset$ for any $U_i \in \mathcal{U}$, then X is connected.

Denote $V_1 = S^1 - \{(0, -1)\}$ and $V_2 = S^1 - \{(0, +1)\}$. Note that $v_1|_{V_1} : V_1 \to v_1(V_1)$ and $\pi|_{v_1(V_1)} : v_1(V_1) \to V_1$ are inverse, because v_1 are local sections of E over S^1(meaning that v_1 is injective). So as $v_2|_{V_2}$ and $\pi|_{v_2(V_2)}$. π^{-1} is continuous and $\pi^{-1}(V_i)$ is connected, so $\{\pi^{-1}(V_i)\}$ is a connected covering of E. Then we have $\pi^{-1}(V_1) \cup \pi^{-1}(V_2) = \pi^{-1}(V_1 \cup V_2) = \pi^{-1}(S^1) = E$. Define $H = \{(b, c)|b > 0\} \subset V_1 \cap V_2$ is a connected subset. We've proved $v_i t_{ij} = v_j$ and $t_{ij} = 1$ for $b > 0$. So $v_1(H) = v_2(H) =: v(H)$. $v(H) \cap \pi^{-1}(V_i) \neq \emptyset$, $i = 1, 2$. Using the property above, E is connected. Thus E is a hopf bundle. □

We summarize above discussion by the following theorem:

Theorem 4.6. Let

$$A(a,b,c) = \begin{bmatrix} a+c & b \\ b & a-c \end{bmatrix}, \text{ which has eigenvalues } \lambda_{\pm} = a \pm \sqrt{c^2+b^2}$$

be a symmetric real matrix where $(a,b,c) \in \mathbb{R}^3$. Then there is a S^0-bundle over $\mathbb{R}^3 - \{(a,0,0)|a \in \mathbb{R}\}$ with fiber being the eigenspace to the first wigenvalues. Then this bundle over any loops enclose $\hat{a}$-axis is a hopf bundle while over the loop not enclose $\hat{a}$-axis is a trivial bundle, see Fig3.

Replacing *first eigenvalues* to *second eigenvalues*, the statement is also true. □

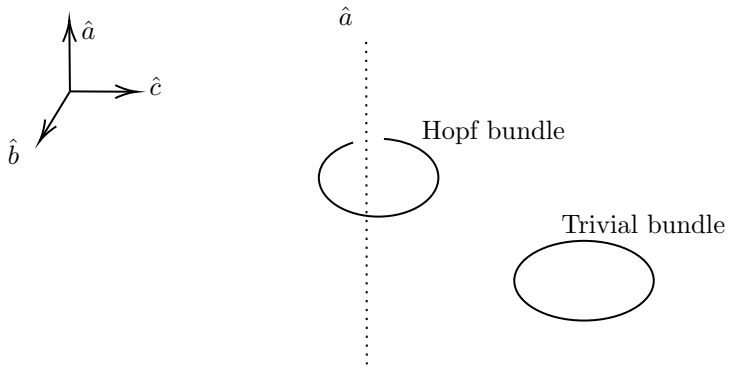

Figure 3: 2-band Hermitian Hamiltonian

It leads to that the eigenvector of first (resp. second) eigenvector turn to its inverse after the parameter evolves along the whole round of the loop enclosing $\hat{a}$-axis. A summary is in table1.

Loop	Enclose $\hat{a}$	Not enclose $\hat{a}$
bundle of first/second eigenspace	hopf	trivial
state of first/second eigenvector after rotation around the loop	inverse	initial

Table 1: classifying of loops

4.2 Classifying II: Fundamental group of moduli space

In classifying I, we consider two eigenvectors separately, which is useful when two eigenvectors have high symmetry. In this section, we provide the second classification considering two eigenvectors simultaneously.

In order to more clearly represent the underlying physical meaning, we introduce a different notation from that employed in the previous section.

We denote eigenvetor associated to eigenvalue $\omega_\pm$ by $\phi_\pm$.

Recall any Hermitian 2×2 matrix H can be represented by Pauli matrix:

$$\sigma_1 = \begin{bmatrix} 0 & 1 \\ 1 & 0 \end{bmatrix}, \sigma_2 = \begin{bmatrix} 0 & -i \\ i & 0 \end{bmatrix}, \sigma_1 = \begin{bmatrix} 1 & 0 \\ 0 & -1 \end{bmatrix}$$

i.e., $H_2 = f_0 I + f_1\sigma_1 + f_2\sigma_2 + f_3\sigma_3$

With PT-symmetry (to make H_2 real), $f_2 = 0$. So the Hamiltonian takes the form

$$H_2 = \begin{bmatrix} f_0 + f_3 & f_1 \\ f_1 & f_0 - f_3 \end{bmatrix}$$

Its eigenvalues and eigenvectors are:

$$(f_1 \neq 0)\, \omega_- = f_0 - \sqrt{{f_1}^2 + {f_3}^2}, \quad \omega_+ = f_0 + \sqrt{{f_1}^2 + {f_3}^2}$$

$$\phi_- = \begin{bmatrix} -\frac{-f_3 + \sqrt{{f_1}^2+{f_3}^2}}{f_1} \\ 1 \end{bmatrix}, \quad \phi_+ = \begin{bmatrix} -\frac{-f_3 - \sqrt{{f_1}^2+{f_3}^2}}{f_1} \\ 1 \end{bmatrix}$$

$$(f_1 = 0, f_3 < 0)\, \omega_- = f_0 - |f_3|, \quad \omega_+ = f_0 + |f_3|$$

$$\phi_- = \begin{bmatrix} 1 \\ 0 \end{bmatrix}, \quad \phi_+ = \begin{bmatrix} 0 \\ 1 \end{bmatrix}$$

$$(f_1 = 0, f_3 > 0)\, \omega_- = f_0 - |f_3|, \quad \omega_+ = f_0 + |f_3|$$

$$\phi_- = \begin{bmatrix} 0 \\ 1 \end{bmatrix}, \quad \phi_+ = \begin{bmatrix} 1 \\ 0 \end{bmatrix}$$

Since eigenvectors are independent on a, so we assume $a = 0$.

We first depict eigenspace spanned by ϕ_-(blue) and ϕ_+(red) in Fig4, where the short sticks denotes 1-dimensional eigenspaces.

Observation:

- Along the line $f_1 = kf_3$, the system has same eigenvectors.
- This field is a good example for a system that should rotate 4π to return to initial, see Fig5; the blue round is rotating 2π, turning the vector to its inverse; the red round is the second round of rotating 2π, turning the vector to its initial.
- This leads to an interesting phenomenon: eigenvectors swapping. Since rotating π along the loop corresponding to rotating $\pi/2$ of eigenvectors and the angle between $\phi_\pm$ is $\pi/2$, we have the swapping of ϕ_+ and ϕ_- when we "passing through" the origin. See Fig6. Here, the "swap" means the first eigenvector becomes the second eigenvector and the second eigenvector becomes the first eigenvector.

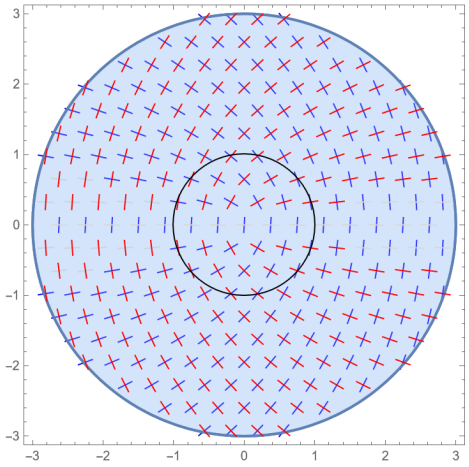

Figure 4: Eigenvector field

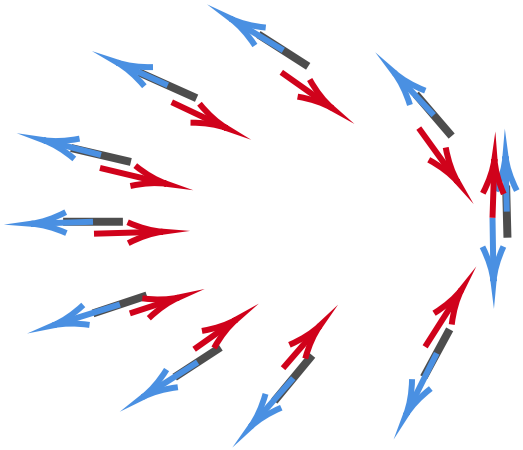

Figure 5: Field of "rotating 4π to initial"

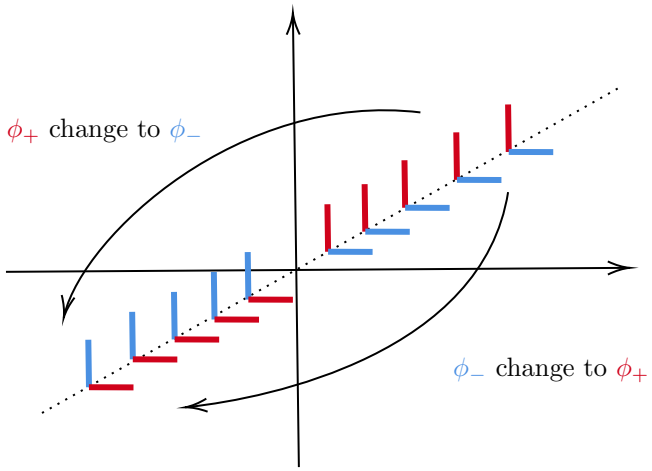

Figure 6: Swap eigenvectors

The eigenvalues do not matter; the order of corresponding eigenvectors matters. So we focus on the ordered pair (ϕ_-, ϕ_+)

Hence, the moduli space is $M_2 := \{(f_3, f_1) \in \mathbb{R}^2\}/\sim$, where the relation $\sim$ is

$$(f_3, f_1) \sim (f_3', f_1') \iff H_2(f_3, f_1) \text{ and } H_2(f_3', f_1') \text{ have same ordered pair } (\phi_-, \phi_+)$$

.

Now the question is to study the topology of M_2.

Property 4.7. $M_2 \simeq S^1$.

Proof. From observation we have (ϕ_-, ϕ_+) coincides on the line, hence we only need to consider H_2 on the unit sphere S^1 in $\mathbb{R}^2$. The following will shows on each point in S^1 we have different (ϕ_-, ϕ_+).

On S^1, let $f_3 = cos\theta$, $f_1 = sin\theta$. The eigenvalues and normalized eigenvectors corresponding to θ are as follows:

$$\omega_- = -1, \omega_+ = 1$$

$$\phi_- = \begin{bmatrix} -\sin(\theta/2) \\ \cos(\theta/2) \end{bmatrix}, \phi_+ = \begin{bmatrix} \cos(\theta/2) \\ \sin(\theta/2) \end{bmatrix}$$

Claim: $\{H_2(f_3, f_1) \,|\, (f_3, f_1) \in S^1\} \xrightarrow{1:1} \overline{(f_3, f_1)} \in M_2$ There are two ways to show it.

(1)Considering $H_2(\phi_-)$:

H_2 can be represented by ϕ_-:

$$H_2 = \begin{bmatrix} f_3 & f_1 \\ f_1 & -f_3 \end{bmatrix} = \begin{bmatrix} \cos\theta & \sin\theta \\ \sin\theta & -\cos\theta \end{bmatrix} = 1 - 2\phi_-{\phi_-}^T$$

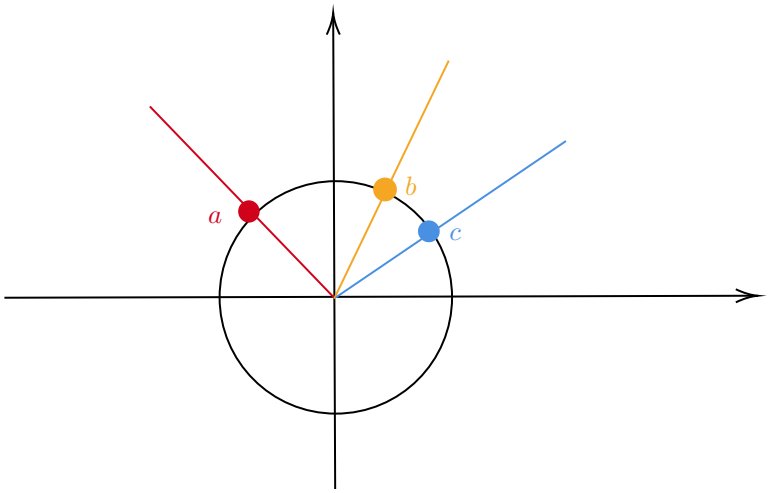

Figure 7: Represent element in S^1

$$\phi_- \in SO(2) \xrightarrow{2:1} H_2(\phi_-) = 1 - 2\phi_-{\phi_-}^T$$

, since $H_2(\phi_-) = H_2(-\phi_-)$. Hence, $M_2 = SO(2)/\mathbb{Z}_2 = S^1/\mathbb{Z}_2 = S^1$

(2)Considering θ:

$$e^{i\theta} \in S^1 \xrightarrow{1:1} \begin{bmatrix} \cos\theta & -\sin\theta \\ \sin\theta & \cos\theta \end{bmatrix} \in SO(2) \xrightarrow{1:1} \theta \in [0, 2\pi) \xrightarrow{1:1} H_2(\theta) = \begin{bmatrix} \cos\theta & \sin\theta \\ \sin\theta & -\cos\theta \end{bmatrix}$$

□

Here is a geometric view: Each point in S^1 repesents an equivalence class in M_2. For example, e.g., a (resp. b,c) represents points (f_3, f_1) on the red (resp. yellow, blue) line(See Fig7).

Conclusion 4.8. $\pi_1(M_2) = \pi_1(S^1) = \mathbb{Z}$.

4.3 Classifying III:$\pi_1(SO(2)/O(1))$

- A two band Hamiltonian is $H_2 = \sum_{j=1}^{2} j \left|u_k^j\right\rangle \left\langle u_k^j\right|$, where $\left|u_k^j\right\rangle$ are eigenvectors by spectrum theorem.
- H_2 can be determined by a set of "right hand" orthonormal vectors $\left|u_k^j\right\rangle$ and unchanged for two of eigenvectors flip:$\left|u_k^j\right\rangle \mapsto -\left|u_k^j\right\rangle$.

Remark 4.9. Note that H_2 remains unchanged for **two** eigenvectors flip, **NOT** one of them. This is because we require all eigenvectors to form a right-hand frame (Any odd number flip will change the determinant from 1 to -1). □

Therefore H_2 can be describe by $SO(2)/O(1) = S^1/\mathbb{Z}/2 = \mathbb{RP}^2$. Then $\pi_1(SO(2)/O(1)) = \mathbb{Z}/2$ characterize all nontrivial loops in this parametrized system.

The visualizing of $\pi_1(SO(2)/O(1)) = \mathbb{Z}/2$ is as following: $SO(2)/O(1)$ is S^1 identifying antipodal points. The generator of $\pi_1(SO(2)/O(1)) = \mathbb{Z}/2$ is depicted in Fig8.

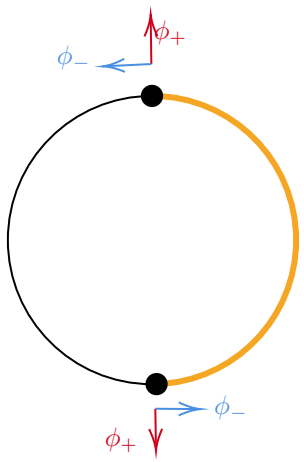

Figure 8: Generator of $\pi_1(SO(2)/O(1))$

Along this loop, the eigenvectors evolves to their inverse.

4.4 Comparison of 3 classifying methods

Topological invariants obtained by classification I, II, and III have different meanings:

- **Classification I:** Two eigenvectors are orthogonal, so we only consider one eigenspace. We identify an normalized eigenvector with its inverse, since we use the language of bundle and the fiber of the bundle is an eigenspace.
- **Classification II:** We distinguish an eigenvector with its inverse.
- **Classification III:** Two eigenvectrs form a right-hand frame, so we can only consider one eigenvector. Quotient $O(1)$ means we identify an normalized eigenvector with its inverse.

We can choose different topological invariants in different cases by physical meaning.

5 3-band Hermitian Hamiltonian over $\mathbb{R}$

- A three band Hamiltonian is $H_k = \sum_{j=1}^{3} j \left|u_k^j\right\rangle \left\langle u_k^j\right|$.
- H_k can be determined by a set of "right hand" orthonormal vectors $\left|u_k^j\right\rangle$ and unchanged for two of eigenvectors flip:$\left|u_k^j\right\rangle \mapsto -\left|u_k^j\right\rangle$.

  Remark 5.1. H_k remains unchanged for two of the eigenvectors flip, not one or three of them, because we need all eigenvectors to form a right-hand frame (Any odd number flips will change the determinant from 1 to -1).
- H_k can be describe by $SO(3)/D_2$.
- It's some kind of eigenbundle of H_k, see Fig9.

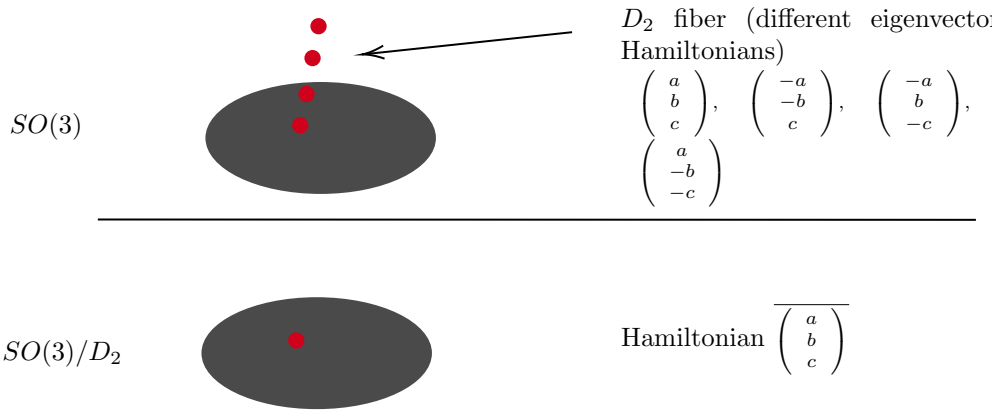

Figure 9: Eigenbundle

5.1 Classifying I: Universal bundles of $D_2 \to SO(3) \to SO(3)/D_2$

Consider the bundle

$$D_2 \hookrightarrow SO(3) \xrightarrow{\pi} SO(3)/D_2 =: X, \quad \pi(x) = \bar{x}$$

Goal: The isomorphism classes of principal D_2-bundles over X are denoted by $Prin_{D_2}(X)$ and $Prin_{D_2}(X) \simeq [X, BD_2]$ where BD_2 is the classifying space of D_2. The following will show which $\phi \in [X, BD_2]$ corresponds to the principal D_2-bundle we considered.

Compute classifying bundle

- The classifying bundle of $O(1)$ is $f : EO(1) = V_1(\mathbb{R}^\infty) \to Gr_1(\mathbb{R}^\infty)$, $f(v) = span(v)$

- Then we can compute the classifying bundle of $D_2 \simeq \mathbb{Z}_2 \times \mathbb{Z}_2 = O(1) \times O(1)$ is $f \times f : V_1(\mathbb{R}^\infty) \times V_1(\mathbb{R}^\infty) \to Gr_1(\mathbb{R}^\infty) \times Gr_1(\mathbb{R}^\infty)$

Remark 5.2. $V_1(\mathbb{R}^\infty)$ is the Stiefel manifold. $V_k(\mathbb{R}^n)$ is the set of all orthonormal k-frames in $\mathbb{R}^n$ i.e., the set of ordered orthonormal k-tuples of vectors in $\mathbb{R}^n$.

We need to find $\phi : X \to Gr_1(\mathbb{R}^\infty) \times Gr_1(\mathbb{R}^\infty)$, such that $\pi : SO(3) \to X$ appears in the pullback of ϕ and $f \times f$:

$$\begin{array}{ccc} SO(3) & \longrightarrow & V_1(\mathbb{R}^\infty) \times V_1(\mathbb{R}^\infty) = ED_2 \\ \downarrow{\scriptstyle \pi} & & \downarrow{\scriptstyle f \times f} \\ X & \xrightarrow[\phi]{} & Gr_1(\mathbb{R}^\infty) \times Gr_1(\mathbb{R}^\infty) = BD_2 \end{array}$$

Orbital of $\begin{bmatrix} a \\ b \\ c \end{bmatrix} \in SO(3)$

where $f : V_1(\mathbb{R}^\infty) \to Gr_1(\mathbb{R}^\infty)$ is defined by $f(v_1) = span(v_1)$.

$$SO\left(3\right) = \{M \in \mathrm{M}_{3\times 3}\left(\mathbb{R}\right) | M^T M = I, \det M = 1\}$$

$$D_2 = \left\{ I, \begin{bmatrix} -1 & & \\ & -1 & \\ & & 1 \end{bmatrix}, \begin{bmatrix} -1 & & \\ & 1 & \\ & & -1 \end{bmatrix}, \begin{bmatrix} 1 & & \\ & -1 & \\ & & -1 \end{bmatrix} \right\} \subset SO\left(3\right)$$

$$\forall \begin{bmatrix} a \\ b \\ c \end{bmatrix} \in SO\left(3\right) \ \left(a, b, c \in M_{1\times 3}\right), \text{the orbital of } \begin{bmatrix} a \\ b \\ c \end{bmatrix} \text{ is } \begin{bmatrix} a \\ b \\ c \end{bmatrix}, \begin{bmatrix} a \\ -b \\ -c \end{bmatrix}, \begin{bmatrix} -a \\ b \\ -c \end{bmatrix}, \begin{bmatrix} -a \\ -b \\ c \end{bmatrix}$$

Construct ϕ

Claim: $\phi : SO(3)/D_2 \to Gr_1(\mathbb{R}^\infty) \times Gr_1(\mathbb{R}^\infty)$ is

$$\phi\left(\overline{\begin{bmatrix} a \\ b \\ c \end{bmatrix}}\right) = \left(span\left(\begin{bmatrix} a & 0 & 0 & \cdots \end{bmatrix}\right), span\left(\begin{bmatrix} b & 0 & 0 & \cdots \end{bmatrix}\right)\right)$$

The pullback of ϕ and $f \times f$ is constructed as

$$S = X \times_{BD_2} ED_2 = \{ \left(\overline{\begin{bmatrix} a \\ b \\ c \end{bmatrix}}, (v_1, v_2) \right) | \overline{\begin{bmatrix} a \\ b \\ c \end{bmatrix}} \in X, (v_1, v_2) \in V_1\left(\mathbb{R}^\infty\right) \times V_1\left(\mathbb{R}^\infty\right),$$

$$span\left(\begin{bmatrix} a & 0 & 0 & \cdots \end{bmatrix}\right) = span\left(v_1\right), span\left(\begin{bmatrix} b & 0 & 0 & \cdots \end{bmatrix} = span\left(v_2\right)\right)\}$$

Since v_1, v_2 are orthonormal, we have $v_1 = [\pm a, 0, 0, \cdots]$, $v_2 = [\pm b, 0, 0, \cdots]$.
It's easy to show $S \simeq SO(3)$

$$\left(\overline{\begin{bmatrix} a \\ b \\ c \end{bmatrix}}, (a,b)\right) \mapsto \begin{bmatrix} a \\ b \\ c \end{bmatrix}, \left(\overline{\begin{bmatrix} a \\ b \\ c \end{bmatrix}}, (-a,b)\right) \mapsto \begin{bmatrix} -a \\ b \\ -c \end{bmatrix},$$

$$\left(\overline{\begin{bmatrix} a \\ b \\ c \end{bmatrix}}, (a,-b)\right) \mapsto \begin{bmatrix} a \\ -b \\ -c \end{bmatrix}, \left(\overline{\begin{bmatrix} a \\ b \\ c \end{bmatrix}}, (-a,-b)\right) \mapsto \begin{bmatrix} -a \\ -b \\ c \end{bmatrix}$$

5.2 Classifying II: A ball equipped information like a bundle

In [18], it is established that $\pi_1(SO(3)/D_2) \simeq Q$. In this section, we aim to provide a visualization of $SO(3)/D_2$ and $\pi_1(SO(3)/D_2)$ to offer an intuitive understanding of how eigenframes rotate.

Definition 5.3. The space of Hamiltonians is defined as: $\mathcal{H} = \{H = u_1^T u_1 + 2u_2^T u_2 + 3u_3^T u_3 | [u_1, u_2, u_3] \in SO(3)/D_2\}$

Remark 5.4. For any $[u_1, u_2, u_3] \in SO(3)$, the following four configurations result in the same Hamiltonian H in $\mathcal{H}$, which explains why we quotient by D_2:
$[u_1, u_2, u_3] \sim [-u_1, -u_2, u_3] \sim [-u_1, u_2, -u_3] \sim [u_1, -u_2, -u_3]$

5.2.1 Visualizasion of $SO(3)/D_2$

Recall that $SO(3) = M \in GL(3, \mathbb{R}) \mid M^T M = I, \det M = 1$, representing rotations that preserve orientation. Another way to describe $SO(3)$ is by using rotation parameters-any rotation can be described by a pair $(\hat{r}, \theta)$ which means rotate along $\hat{r}$ by θ.

Definition 5.5. Let $\phi(\hat{r}, \theta)$ represent a rotation around the axis $\hat{r} \in S^2$ by an angle $\theta \in [0, 2\pi]$. Thus, we can describe $SO(3)$ as:

$$SO(3) = \{\phi(\hat{r}, \theta) | \hat{r} \in S^2, \theta \in [0, 2\pi]\}$$

Next, we aim to reduce the parametrization of $SO(3)$ and visualize it.

Fact 5.6. Two key properties are important to note:
(1)$\phi(\hat{r}, \theta) = \phi(-\hat{r}, 2\pi - \theta)$
(2)Specifically, $\phi(\hat{r}, \pi) = \phi(-\hat{r}, \pi)$

The first fact implies that we can always restrict the parameter θ to the interval $[0, \pi]$. For example, $\phi(\hat{x}, 3\pi/2) = \phi(\hat{x}, 2\pi - 3\pi/2) = \phi(\hat{x}, \pi/2)$.

This leads us to view $SO(3)$ as a solid ball with radius π. Any point $\vec{t}$ in the ball represents the rotation $\phi(\vec{t}/|\vec{t}|, |\vec{t}|)$. For instance, the bold point in Fig. 10 corresponds to $\phi(\hat{y}, \pi/2)$, representing a rotation by $\pi/2$ along the $\hat{y}$ axis.

The second fact suggests that the antipodal points on the boundary of the ball should be identified (Fig. 11).

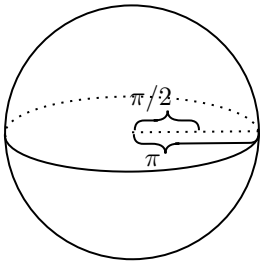

Figure 10: Parametrization of $SO(3)$

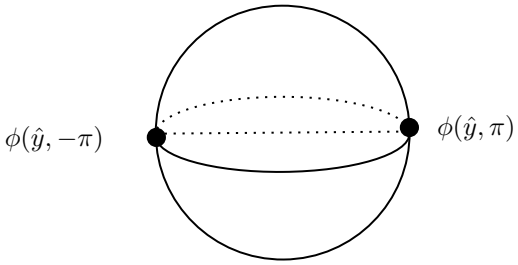

Figure 11: Antipodal points are the same in $SO(3)$

Conclusion 5.7. Therefore, $SO(3)$ can be described as a ball of radius π with antipodal points on the boundary identified. In other words, $SO(3) \simeq B^3(\pi)/\sim$, where $x \sim y$ if $x, y \in \partial B^3(\pi)$ and $x = -y$.

Next, we turn our attention to visualizing $SO(3)/D_2$.

Fact 5.8. The dihedral group D_2 consists of the following elements: $D_2 = \{\phi(\hat{x}, \pi), \phi(\hat{y}, \pi), \phi(\hat{z}, \pi), id\}$. These elements can be represented by the four points shown in Fig. 12.

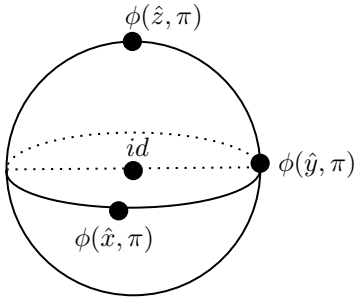

Figure 12: D_2 in $SO(3)$

Conclusion 5.9. $SO(3)/D_2$ is a ball of radius π, with two operations applied:

(1)glue antipodal points
(2)glue four points in Fig12 to a point

Visualize the fundamental group of $SO(3)/D_2$

Fact 5.10. The fundamental group of $SO(3)/D_2$ is isomorphic to the quaternion group Q, i.e., $\pi_1(SO(3)/D_2) \simeq Q = \pm 1, \pm i, \pm j, \pm k$.

Property 5.11. There is a bijection between the following spaces:
$SO(3)/D_2 \leftrightarrow$ space of Hamiltonians $\leftrightarrow$ space of eigenframes
where space of Hamiltonians is defined as in Definition 5.4.

Proof. The bijection is established as follows: $SO(3)/D_2 \leftrightarrow$ {space of Hamiltonians} $\leftrightarrow$ {spaces of eigenframes}
$\phi(\hat{r}, \theta) \mapsto H = u_1^T u_1 + 2u_2^T u_2 + 3u_3^T u_3 \mapsto [u_1, u_2, u_3]$
where $[u_1, u_2, u_3] = \phi(\hat{r}, \theta)[e_1, e_2, e_3]$ and $[e_1, e_2, e_3]$ is the standard frame in $\mathbb{R}^3$.

□

Bu this property, we have following conclusion:

Conclusion 5.12. Any loop in $SO(3)/D_2$ represents the evolution of an eigenframe. Consequently, any element in $\pi_1(SO(3)/D_2)$ can be interpreted as the evolution of an eigenframe.

Here's the rephrased version of your text:

Example 5.13. Consider loops L_1, L_5, and L_6 in Fig. 13, where $\hat{x}$, $\hat{y}$, and $\hat{z}$ correspond to the first, second, and third eigenvectors, respectively.
Evolution of eigenframe on loop L_1: The first eigenvector ($\hat{x}$) remains fixed, while the second ($\hat{y}$) and third ($\hat{z}$) eigenvectors rotate by π.
Evolution of eigenframe on loop L_6: The second eigenvector ($\hat{y}$) stays fixed, with the first ($\hat{x}$) and third ($\hat{z}$) eigenvectors rotating by π.
Evolution of eigenframe on loop L_5: The third eigenvector ($\hat{z}$) is fixed, and the first ($\hat{x}$) and second ($\hat{y}$) eigenvectors rotate by π.

The following example details the computation further.

Example 5.14. Evolution on Loop L_1. Parametrization shown in Fig14.
Referring to [4], the rotation matrix for a rotation by angle ψ around the axis $[a_1, a_2, a_3]$ is given by:

$$\begin{bmatrix} \cos\psi + (1-\cos\psi)\,{a_1}^2 & (1-\cos\psi)\,a_1a_2 - \sin\psi a_3 & (1-\cos\psi)\,a_1a_3 + \sin\psi a_2 \\ (1-\cos\psi)\,a_1a_2 + \sin\psi a_3 & \cos\psi + (1-\cos\psi)\,{a_2}^2 & (1-\cos\psi)\,a_2a_3 - \sin\psi a_1 \\ (1-\cos\psi)\,a_1a_3 - \sin\psi a_2 & (1-\cos\psi)\,a_2a_3 + \sin\psi a_1 & \cos\psi + (1-\cos\psi)\,{a_3}^2 \end{bmatrix}$$

In this case, $a_1 = 0$, $a_2 = \cos\theta$, $a_3 = \sin\theta$, and $\psi = \pi$. Therefore, the rotation matrix (i.e., the eigenframes) becomes:

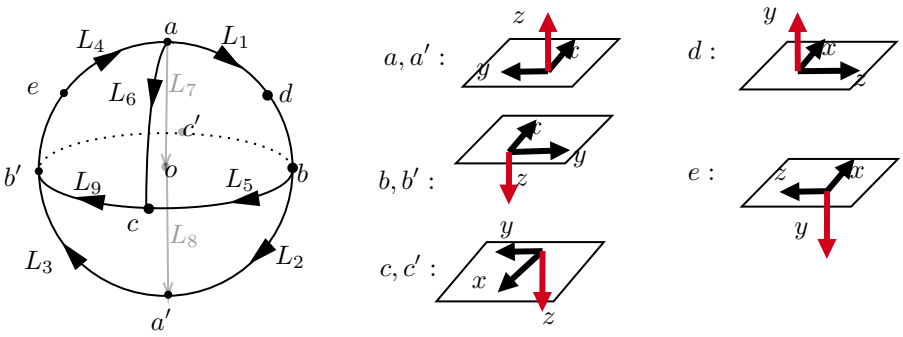

Figure 13: loops in $SO(3)/D_2$

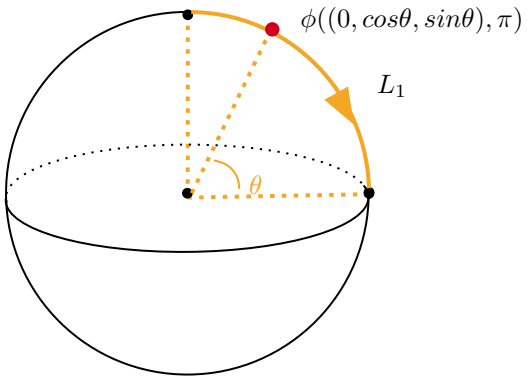

Figure 14: loop L_1

$$\begin{bmatrix} -1 & 0 & 0 \\ 0 & \cos 2\theta & \sin 2\theta \\ 0 & \sin 2\theta & -\cos 2\theta \end{bmatrix}$$

which is parametrized by θ. Hence, the evolution of the eigenframe on loop L_1 involves the first eigenvector ($\hat{x}$) remaining fixed, while the second ($\hat{y}$) and third ($\hat{z}$) eigenvectors rotate by π.

The eight points in Fig. 15 represent a single point, and since loops must start and end at the same point, we only need to consider the loops shown in Fig. 15.

Conclusion 5.15. All non-trivial loops can be represented by the loops (yellow lines) in Fig. 15. (Arrows are omitted for simplicity.)

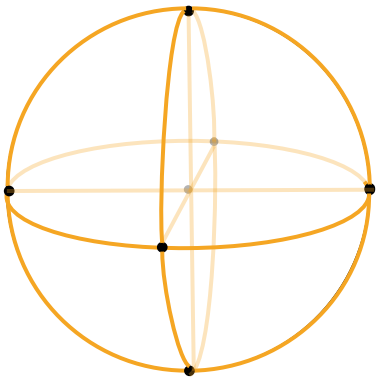

Figure 15: "Base loops" in $SO(3)/D_2$

To explain $\pi_1(SO(3)/D_2)$, the following properties are clear:

- $L_1 = L_4$. Indeed, in L_1, $\hat{y}$ and $\hat{z}$ rotate clockwise, while in L_4^{-1}, $\hat{y}$ and $\hat{z}$ rotate counterclockwise. Hence, $L_1 = (L_4^{-1})^{-1} = L_4$

  Corollary 5.16. $L_1 = L_2 = L_3 = L_4$

  Proof. By step(2) of Conclusion 5.10, we have $L_3 = L_1$ and $L_2 = L_4$. With $L_1 = L_4$, we have $L_1 = L_2 = L_3 = L_4$. □

  Corollary 5.17. The order $|L_1| = 4$

  Proof. $L_1^4 = L_1L_2L_3L_4$ =trivial loop and obviously $L_1^2, L_1^3 \neq$ trivial loop. □

  Corollary 5.18. $L_1^2 = -1$

  Proof. $L_1^4 = 1$ so $L_1^2 = -1$ □

- Similarly, $L_7 = L_8$, and $|L_7| = 4$. Thus, we only need to focus on the 1/8 ball. Since it's known that $\pi_1(SO(3)/D_2) \simeq Q$, the visualization of $\pi_1(SO(3)/D_2)$ is shown in Fig. 16.

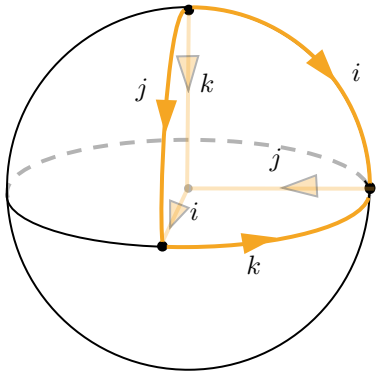

Figure 16: $\pi_1(SO(3)/D_2)$

Remark 5.19. Note that I have selected specific elements to illustrate properties. For instance, if we prove that $L_1 = L_2$, we also have $L_5 = L_9$ in Fig. 13.

Reasonable Guess: When two eigenvectors rotate by π, a degeneracy occurs between these two bands. Furthermore, orientations should be taken into account. For example, on L_1 (or L_2), the eigenvectors $\hat{y}$ and $\hat{z}$ rotate by π, so L_1 (or L_2), being a loop of charge i, encloses a degeneracy between the second and third bands with positive orientation. In contrast, L_1^{-1} encloses a degeneracy between the second and third bands with negative orientation.

Remark 5.20. For the loop -1, although the eigenframe evolution ends at its initial state, this is not a trivial loop. It is similar to a spin in physics, which must rotate by 4π to return to its initial state. A 2π rotation results in $-1 \neq 1$.

Relationship between [1,Fig.3A to C] "Two NLs of the same orientation between the same pair of bands are described by -1" [18]. With this guess, the loop L_1L_2 encloses two degeneracies with the same orientation formed by the second and third bands. Therefore, L_1L_2 has a charge of -1. A similar analysis shows that L_7L_8 encloses two degeneracies with the same orientation formed by the first and second bands. The transformation in [1, Fig. 3A to C] represents the deformation from L_7L_8 to L_1L_2 on our ball, i.e., from $k^2 = -1$ to $i^2 = -1$ (see Fig. 14(b)).

Further discussion

This visualization is valuable because the $SO(3)/D_2$ ball captures the rotational behaviors of frames within a loop, functioning similarly to a bundle. It presents a compelling image.

In the non-Hermitian case, if we could identify a group whose loop encompasses both the evolution of Hermitian and the evolution of eigenframes, we could apply the same approach. However, finding such a group appears to be quite challenging.

6 2-band real pseudo-Hermitian

In this section, we give a different way to recover results in [12], and this method can generalize to the discussion for 3-band real pseudo-Hermitian.

Definition 6.1. Let $\eta = diag[-1, 1]$. A 2-band real pseudo-Hermitian Hamiltonian is a 2×2 real matrix H satisfying $\eta H \eta = H^\dagger$. □

Computation 6.2. Let $H = \begin{bmatrix} a & b \\ c & d \end{bmatrix}$. $\eta H \eta = H^\dagger$ leads to $\begin{bmatrix} a & -b \\ -c & d \end{bmatrix} = \begin{bmatrix} a & c \\ b & d \end{bmatrix}$. □

Conclusion 6.3. Any 2-band real pseudo-Hermitian H has the form

$$H = \begin{bmatrix} a & b \\ -b & c \end{bmatrix} \quad , \quad a, b, c \in \mathbb{R}$$

□

Next, we want to compute the eigenvalues and eigenvectors.

Computation 6.4. The parametrized eigenpolynomial is $\lambda^2 - (a+c)\lambda + ac + b^2 = 0$.

The eigenvalues are $\lambda_\pm = \frac{a+c \pm \sqrt{(a-c-2b)(a-c+2b)}}{2}$

For $b \neq 0$, the eigenvector $v_\pm$ to $\lambda_\pm$ is

$$v_\pm = \begin{bmatrix} \frac{c-\lambda_\pm}{b} \\ 1 \end{bmatrix} = \begin{bmatrix} \frac{c-a \mp \sqrt{(a-c-2b)(a-c+2b)}}{2b} \\ 1 \end{bmatrix}$$

For $b = 0$, $\lambda_+ = max\{a, c\}$, $\lambda_- = min\{a, c\}$. And we have

- $a > c$

$$v_+ = \begin{bmatrix} x \\ 0 \end{bmatrix} \quad , \quad x \in \mathbb{R}, \quad v_- = \begin{bmatrix} 0 \\ y \end{bmatrix} \quad , \quad y \in \mathbb{R}$$

- $c > a$

$$v_+ = \begin{bmatrix} 0 \\ x \end{bmatrix} \quad , \quad x \in \mathbb{R}, \quad v_- = \begin{bmatrix} y \\ 0 \end{bmatrix} \quad , \quad y \in \mathbb{R}$$

- $a = c$, eigenspace to the eigenvector has dimension 2.

□

From the computation, we have

Conclusion 6.5. The degeneracy surfaces (surface at which has only one eigenvalue) are $a-c-2b=0$, and $a-c+2b=0$. These two planes intersect at line $l=\{(x,0,x)|x\in\mathbb{R}\}$ □

We want to compute the configuration of the eigenvectors. Let's consider the eigenvector v_+ firstly. The main idea is to find points that have same v_+.

Computation 6.6. Compute how parameter c affects eigenvectors.
Let $c=s$ where $s\in\mathbb{R}$ is fixed. Then, we find that

- $b\neq 0$

$$v_+(a+s,b,s)=\begin{bmatrix} \frac{s-(a+s)\mp\sqrt{(a+s-s-2b)(a+s-s+2b)}}{2b} \\ 1 \end{bmatrix}$$
$$=\begin{bmatrix} \frac{-a\mp\sqrt{(a-2b)(a+2b)}}{2b} \\ 1 \end{bmatrix}=v_+(a,b,0)$$

- For $b=0, a+s>c=s$, this leads to $a>0$. Hence, $v_+(a+s,0,s)=v_+(a,0,0)$.
- For $b=0, s=c>a+s$, this leads to $0>a$. Hence, $v_+(a+s,0,s)=v_+(a,0,0)$.

□

Conclusion 6.7. (i)We have $v_+(a+s,b,s)=v_+(a,b,0)$, that means, the configuration of v_+ has symmetry of translation $c=s$ plane along the singular line $l=\{(x,0,x)|x\in\mathbb{R}\}$
(ii) By symmetry of translation, we reduce the case to $c=0$ plane.

Computation 6.8. Compute the configuration on the line $a=kb$ for a fixed $k\in\mathbb{R}$
By above conclusion, we only consider $c=0$.

- $b>0$

$$v_+=\begin{bmatrix} \frac{-a-\sqrt{a^2-4b^2}}{2b} \\ 1 \end{bmatrix}=\begin{bmatrix} -\frac{k}{2}-\sqrt{\frac{k^2}{4}-1} \\ 1 \end{bmatrix}$$

- $b<0$

$$v_+=\begin{bmatrix} \frac{-a-\sqrt{a^2-4b^2}}{2b} \\ 1 \end{bmatrix}=\begin{bmatrix} -\frac{k}{2}+\sqrt{\frac{k^2}{4}-1} \\ 1 \end{bmatrix}$$

- $b=0$, $a>0$

$$v_+=\begin{bmatrix} x \\ 0 \end{bmatrix}\quad,\quad x\in\mathbb{R}$$

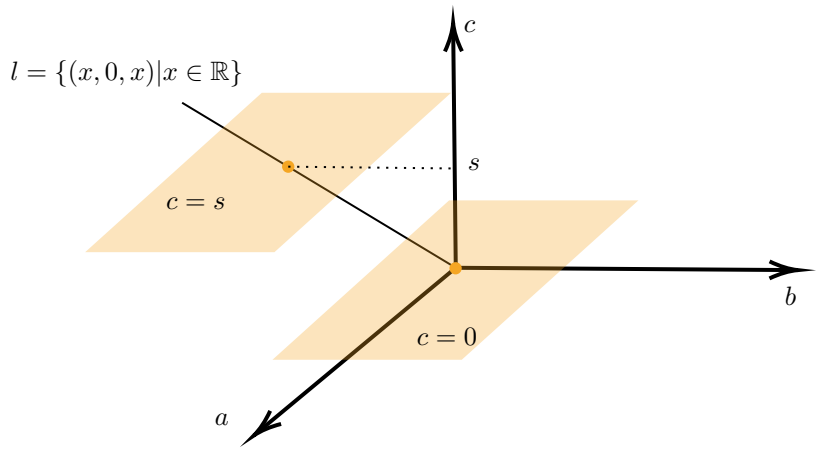

Figure 17: Symmetry of translation

- $b = 0,\ 0 > a$

$$v_+ = \begin{bmatrix} 0 \\ x \end{bmatrix} \quad , \quad x \in \mathbb{R}$$

Computation 6.9. Compute limit at a-axis

- $b > 0,$

$$\lim_{k \to +\infty} -\frac{k}{2} - \sqrt{\frac{k^2}{4} - 1} = \lim_{k \to +\infty} -\left(\frac{k}{2} + \sqrt{\frac{k^2}{4} - 1}\right) = -\infty$$

- $b > 0,$

$$\lim_{k \to -\infty} -\frac{k}{2} - \sqrt{\frac{k^2}{4} - 1} = \lim_{k \to -\infty} \frac{\left(-\frac{k}{2} - \sqrt{\frac{k^2}{4} - 1}\right)\left(-\frac{k}{2} + \sqrt{\frac{k^2}{4} - 1}\right)}{-\frac{k}{2} + \sqrt{\frac{k^2}{4} - 1}} = \lim_{k \to -\infty} \frac{1}{-\frac{k}{2} + \sqrt{\frac{k^2}{4} - 1}} = 0^+$$

- $b < 0,$

$$\lim_{k \to +\infty} -\frac{k}{2} + \sqrt{\frac{k^2}{4} - 1} = \lim_{k \to +\infty} \frac{\left(-\frac{k}{2} + \sqrt{\frac{k^2}{4} - 1}\right)\left(\frac{k}{2} + \sqrt{\frac{k^2}{4} - 1}\right)}{\frac{k}{2} + \sqrt{\frac{k^2}{4} - 1}} = \lim_{k \to +\infty} \frac{-1}{\frac{k}{2} + \sqrt{\frac{k^2}{4} - 1}} = 0^-$$

- $b < 0,$

$$\lim_{k \to -\infty} -\frac{k}{2} + \sqrt{\frac{k^2}{4} - 1} = +\infty$$

By computation of the limit at a-axis, we have conclusions:

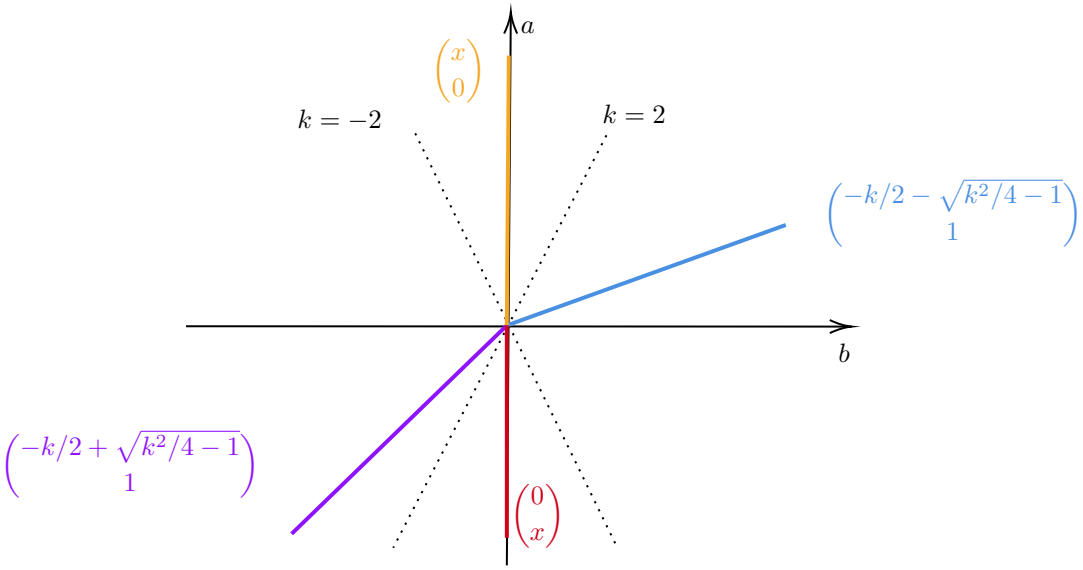

Figure 18: Configuration

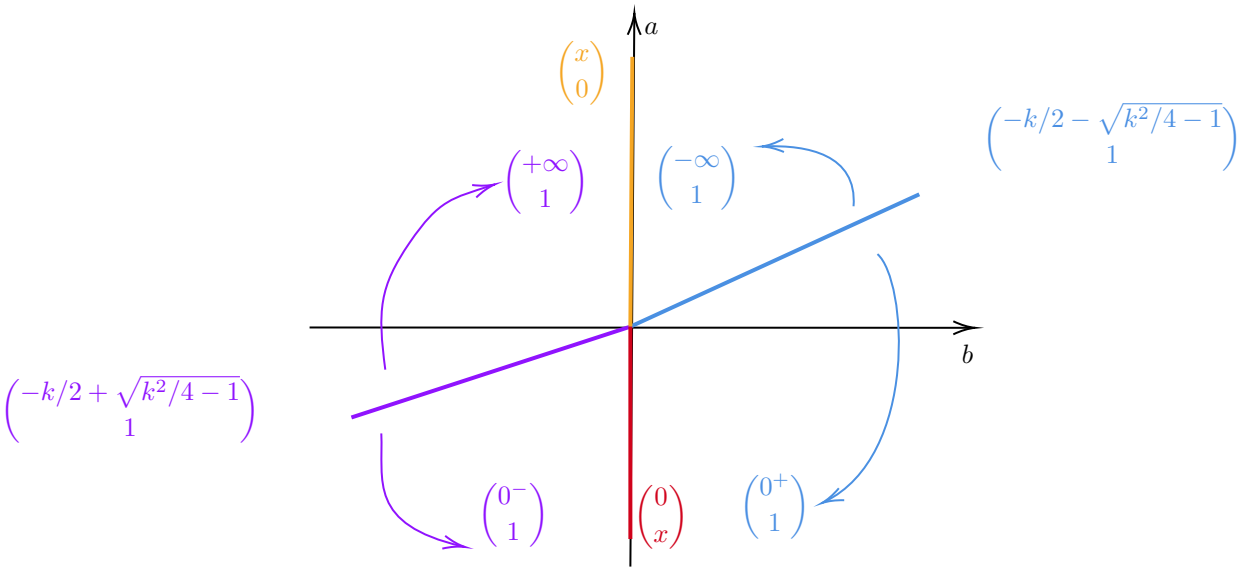

Figure 19: limit at a-axis

Conclusion 6.10. The eigenvector v_+ varies continuously on $\mathbb{R}^2 - \{(a,0,0)|a > 0\}$. Configuration near a-axis (first component is real) can be seen in Fig19 and configuration at the region where the first component is complex can be seen in Fig20.

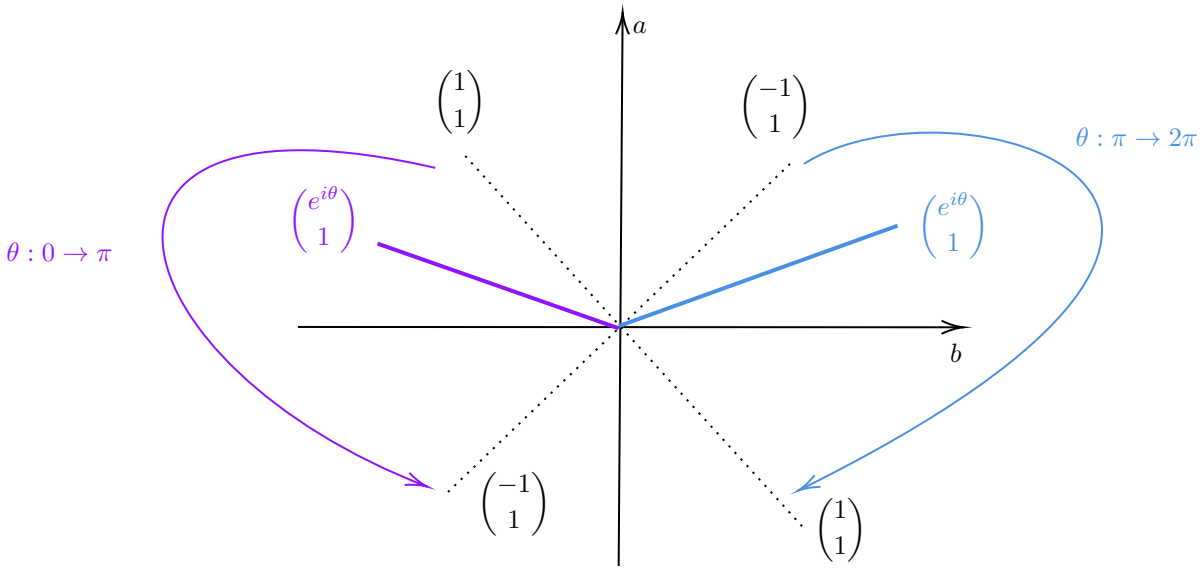

Figure 20: Complex region rotation

Conclusion 6.11. The configuration of eigenvectors is S^1 identifies $A_1 \sim A_2$, $B_1 \sim B_2$ in Fig**??**, which is the space $S^1 \vee S^1 \vee S^1$.

So $\pi_1(S^1 \vee S^1 \vee S^1) = \mathbb{Z} * \mathbb{Z} * \mathbb{Z}$ classifies the singularity, coincides the result in [12].

7 Reducing number of parameters in 3-band real pseudo-Hermitian

In this section we reduce parameter space $\mathbb{R}^6$ of 3-band real psuedo Hermitian matrix to $\mathbb{R}^4$ by symmetry of eigenpolynomials.

Definition 7.1. Let $\eta = diag[-1,1,1]$. The 3-band real psuedo Hermitian H is a 3×3 matrix H satisfying $\eta H \eta = H^\dagger$.

□

Computation 7.2. $\eta \begin{bmatrix} a & b & c \\ d & e & f \\ g & h & l \end{bmatrix} \eta = \begin{bmatrix} a & -b & -c \\ -d & e & f \\ -g & h & l \end{bmatrix} = \begin{bmatrix} a & d & g \\ b & e & h \\ c & f & l \end{bmatrix}$

□

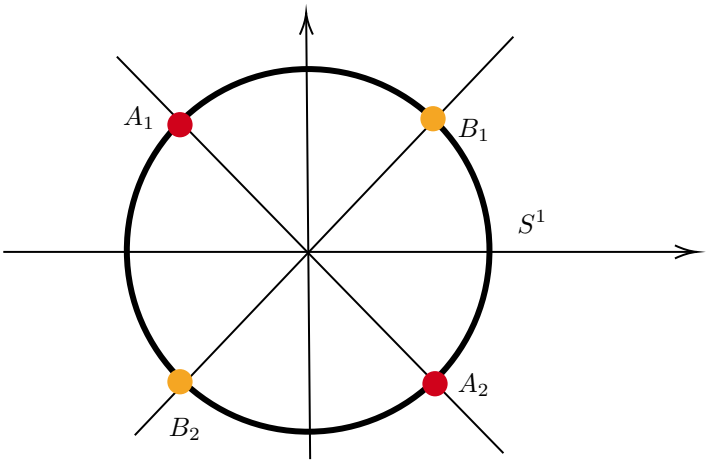

Figure 21: S^1 identifies $A_1 \sim A_2$, $B_1 \sim B_2$

Conclusion 7.3. The 3-band real psuedo Hermitian H is of the form

$$\begin{bmatrix} a & b & c \\ -b & d & e \\ -c & e & f \end{bmatrix} a, b, c, d, e, f \in \mathbb{R}$$

□

Computation 7.4. Translation symmetry

The eigen function of H is

$$(a-\lambda)(d-\lambda)(f-\lambda) + b^2(f-\lambda) + c^2(d-\lambda) - e^2(a-\lambda) - 2bce = 0 \quad (1)$$

The eigenvector is the solution to

$$\begin{bmatrix} a-\lambda & b & c \\ -b & d-\lambda & e \\ -c & e & f-\lambda \end{bmatrix} \begin{bmatrix} x_1 \\ x_2 \\ x_3 \end{bmatrix} = \begin{bmatrix} 0 \\ 0 \\ 0 \end{bmatrix}$$

Consider the transformation $(a, b, c, d, e, f) \to (a' = a + s, b, c, d' = d + s, e, f' = f + s)$.

Then the eigen function becaomes

$(a+s-\lambda')(d+s-\lambda')(f+s-\lambda') + b^2(f+s-\lambda') + c^2(d+s-\lambda') - e^2(a+s-\lambda') - 2bce = (a-(\lambda'-s))(d-(\lambda'-s))(f-(\lambda'-s)) + b^2(f-(\lambda'-s)) + c^2(d-(\lambda'-s)) - e^2(a-(\lambda'-s)) - 2bce = 0$ (2)

Comparison with (1) and (2), we have $\lambda' - s = \lambda$.

Therefore, the equation

$$\begin{bmatrix} a+s-\lambda' & b & c \\ -b & d+s-\lambda' & e \\ -c & e & f+s-\lambda' \end{bmatrix} \begin{bmatrix} x_1 \\ x_2 \\ x_3 \end{bmatrix} = \begin{bmatrix} 0 \\ 0 \\ 0 \end{bmatrix}$$

is equal to the equation

$$\begin{bmatrix} a-\lambda & b & c \\ -b & d-\lambda & e \\ -c & e & f-\lambda \end{bmatrix} \begin{bmatrix} x_1 \\ x_2 \\ x_3 \end{bmatrix} = \begin{bmatrix} 0 \\ 0 \\ 0 \end{bmatrix}$$

That means, translation preserves eigenspace.

Computation 7.5. Strech symmetry

Consider the transformation $(a, b, c, d, e, f) \to (ka, kb, kc, kd, ke, kf)$ when $k \neq 0$.

The eigen function becomes

$$(ka-\lambda')(kd-\lambda')(kf-\lambda')+k^2b^2(kf-\lambda')+k^2c^2(kd-\lambda')-k^2e^2(ka-\lambda')-2k^3bce = 0$$

Devide it by k^3, we obtain

$$(a-\lambda'/k)(d-\lambda'/k)(f-\lambda'/k)+b^2(f-\lambda'/k)+c^2(d-\lambda'/k)-e^2(a-\lambda'/k)-2bce = 0$$

Comparison with (1), we have $\lambda'/k = \lambda$.

Therefore,

$$\begin{bmatrix} ka-\lambda' & kb & kc \\ -kb & kd-\lambda' & ke \\ -kc & ke & kf-\lambda' \end{bmatrix} \begin{bmatrix} x_1 \\ x_2 \\ x_3 \end{bmatrix} = \begin{bmatrix} 0 \\ 0 \\ 0 \end{bmatrix}$$

has same solution as

$$\begin{bmatrix} a-\lambda & b & c \\ -b & d-\lambda & e \\ -c & e & f-\lambda \end{bmatrix} \begin{bmatrix} x_1 \\ x_2 \\ x_3 \end{bmatrix} = \begin{bmatrix} 0 \\ 0 \\ 0 \end{bmatrix}$$

by primary row transformation.

Hence, strech transformation preserves eigenspace.

Conclusion 7.6. (i) $v_i(a+s, b, c, d+s, e, f+s) = v_i(a, b, c, d, e, f)$, $i = 1, 2, 3$

(ii) $v_i(ka, kb, kc, kd, ke, kf) = v_i(a, b, c, d, e, f)$, $k \neq 0$, $i = 1, 2, 3$

By above conclution, we can always set one of a, d, f to 0 and one of other elements to 1. This reduce parameters from $\mathbb{R}^6$ to $\mathbb{R}^4$, which is helpful for further works.

8 Intersection homology of the base space

The previous section do not intersect the singular points in the base space of the bundle (parameter space). In this section, we study the topology of the base space by intersection homology.

8.1 Intersection homology

In recent years, intersection homology has become an indispensable tool for studying the topology of singular spaces. While the main results of usual homology theories often fail for singular spaces, intersection homology effectively recovers these properties, bridging this critical gap. Appropriate reference for intersection homology/homotopy are [5],[3]

Definition 8.1. A filtration is a sequence of closed subsets of X:
$X^n \supseteq X^{n-1} \supseteq \cdots \supseteq X^2 \supseteq X^1 \supseteq X^0 \supseteq X^{-1}$
The connected component of $X^i - X^{i-1}$ is called stratum.

- In application, X^i is always i-dimension singularities of X
- A stratum in $X^i - X^{i-1}$ can be view as i-dimension spaces without lower dimensional singularities.

Let X be a filtered simplicial complex. We say i-simplex σ in general position of stratum S if $dim(\sigma \cap S) \leqslant dim(\sigma) + dim(S) - n$ for every stratum S of X

It is always possible for us to move an i-simplex to be in a general position with stratum S in manifolds. However, this is not true in singular spaces.

Definition 8.2. Let X be filtered space of formal dimension n. Let $\mathcal{F}$ be the set of strata of X. A perversity on X is a function $\bar{p} : \mathcal{F} \to \mathbb{Z}$ such that $\bar{p}(S) = 0$ if $S \subset X^n - X^{n-1}$

Definition 8.3. i-simplex σ is called $\bar{p}$-allowable if $dim(\sigma \cap S) \leqslant dim(\sigma) + dim(S) - n + \bar{p}(S)$ for every stratum S of X

We tolerate to what extent the strangeness of the i-simplex; if it is too strange, we do not acknowledge it as an allowed i-chain, but if it is not too strange, we accept it as an allowable i-simplex.

Definition 8.4. Let X be a filtered simplicial simplex with filtration $X_n \supset X_{n-2} \supset \cdots \supset X_0$.

An i-chain ζ is called $\bar{p}$-allowable if every simplex in ζ and $\partial\zeta$ is $\bar{p}$-allowable.

Define the group $I_pC_i(X)$ be the subset of $C_i(X)$ consisting of $\bar{p}$-allowable i-chains.

It can be shown that the chain complex $(C_*(X), \partial)$ restricts to a chain complex $(I_pC_*(X), \partial)$.

Definition 8.5. The intersection homology groups are defined by $I_pH_i(X) = H_i(I_pC_\cdot(X))$

For a topological space, we need PL intersection homology which is independent of triangulation. Let's define PL homology first.

Definition 8.6. The simplicial complex K' is a *subdivision* of K if:

- $|K| = |K'|$

- Every simplex of K' is contained in some simplex of K

Definition 8.7. A triangulation T of a topological space X is a pair $T = (K, h)$ where

- K is a locally finite simplicial complex
- $h : |K| \to X$ is a homeomorphism

Remark 8.8. Locally finite means: For all $x \in |K|$, there exists a neighborhood U such that U intersects only finitely many simplices.

Definition 8.9. Let $T = (K, h)$ and $S = (L, j)$ be two triangulations. We say T is equivalent to S if and only if $j^{-1}h$ is a simplicial isomorphism.

Definition 8.10. A subdivision of $T = (K, h)$ is a pair $T' = (K', h)$, where K' is a subdivision of K.

Definition 8.11. A PL (piecewise linear) space is a topological space X with

$$\mathcal{T} = \{\text{locally finite triangulations}\}$$

such that:

- For every $T \in \mathcal{T}$, every subdivision of T is also in $\mathcal{T}$.
- For every $T, S \in \mathcal{T}$, T and S have a common refinement.

Remark 8.12. Let $T = (K, h)$ and $S = (L, j)$. T, S have a common refinement means: there exists a subdivision $T' = (K', k)$ of T and a subdivision $S' = (L', \ell)$ of S such that the induced map $f : K' \to L'$ is a simplicial isomorphism.

Construction 8.13. We define a relation $\leqslant$ on $\mathcal{T}$ as following: Let $T = (K, h),\ S = (L, l) \in \mathcal{T}$

Define $T \leq S \iff S$ equivalent to a subdivision of T.

Fact 8.14. $(\mathcal{T}, \leq)$ is a directed set (i.e., the relationship $\leqslant$ satisfying (1) transitive (2) reflexive (3) for any T, $S \in \mathcal{T}$, $\exists W \in \mathcal{T}$ such that $T \leqslant W$ and $S \leqslant W$)

Definition 8.15. Let $(X, \mathcal{T})$ be a PL space. For $T = (K, k) \in \mathcal{T}$, define $C_*^T(X) = C_*(|K|)$.

Definition 8.16. Let $T = (K, k) \leqslant T' = (K', k')$ in $\mathcal{T}$, we want to define a map $C_*^T(X) \to C_*^{T'}(X)$, called subdivision chain map as following:

$$C_*^T(X) = C_*(|K|) \longrightarrow C_*(|K'|) = C_*^{T'}(X), \quad \sigma \mapsto \sum_{\tau_\sigma \subseteq |\sigma|} \tau_\sigma$$

For $\xi = \sum_i a_i \sigma_i$, the map is

$$\xi \mapsto \sum_i a_i \sum_{\tau_{\sigma_i} \subseteq |\sigma_i|} \tau_{\sigma_i}$$

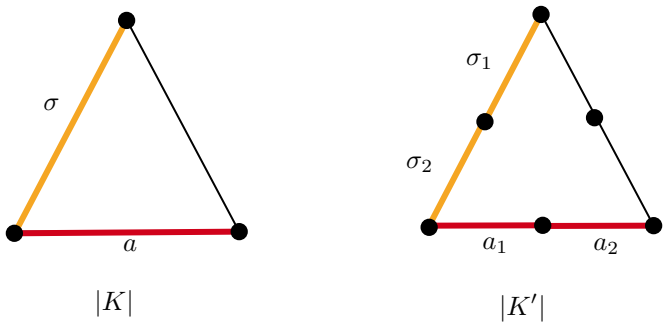

Figure 22: An example for subdivision chain map

Example 8.17.

$$\sigma \mapsto \sigma_1 + \sigma_2$$

$$\sigma + 2a \mapsto \sigma_1 + \sigma_2 + 2(a_1 + a_2)$$

It's easy to check that with above data, we can define a direct limit as following:

Definition 8.18. $C_*^{\mathcal{T}}(X) := \varinjlim_{T \in \mathcal{T}} C_*^T(X)$, where $C_*^T(X) = C_*(|K|)$ for $T = (K, k)$

Actually, we do not need all triangulations in $\mathcal{T}$. We only need a subset of $\mathcal{T}$ containing all subdivisions of a fixed triangulation T_0.

Property 8.19. Let X be a PL space with admissible triangulation $\mathcal{T}$. Let $T_0 = (K, k) \in \mathcal{T}$ and let $\mathcal{T}_0$ be the subset of $\mathcal{T}$ consisting of subdivision of T_0. Then $C_*^{\mathcal{T}}(X) = \varinjlim_{T \in \mathbb{T}} C_*^T(X) \cong \varinjlim_{T \in \mathbb{T}_0} C_*^T(X)$.

Definition 8.20. X is a PL space. Define PL homology of PL space $(X, \mathcal{T})$ as $\mathcal{H}_*(X) := H_*(C_\bullet^{\mathcal{T}}(X))$

Property 8.21. Let X be a PL space. Then $\mathcal{H}_*(X) \cong H_*(X)$, where $H_*(X)$ can be singular or simplicial homology with respect to any triangulations.

Remark 8.22. PL intersection homology (defined later) may not isomorphic to$H_*(X)$ in general!

Next, we can define PL intersection homology.

Definition 8.23. Let X be a PL filtered space such that every skeleton X^i is a subcomplex of any admissible triangulation.

Define $I^{\bar{p}}C_*^{\mathcal{T}}(X) := \varinjlim_{T \in \mathcal{T}} I^{\bar{p}}C_*^T(X)$, where $I^{\bar{p}}C_*^T(X) := I^{\bar{p}}C_*(|K|)$.

Remark 8.24. Filtration and perversity of X can "move to" $|K|$ by homeomorphism k.

Fact 8.25. If $T \leq T'$, the subdivision chain map $\bar{\nu} : C_*^T(X) \to C_*^{T'}(X)$ restricts to a map $\nu : I^{\bar{p}}C_*^T(X) \to I^{\bar{p}}C_*^{T'}(X)$

Definition 8.26. We define the PL intersection homology of PL space $(X, \mathcal{T})$ as $I^{\bar{p}}\mathcal{H}_*(X) := H_*(I^{\bar{p}}C_\bullet^{\mathcal{T}}(X)) \cong \varinjlim_{T \in \mathcal{T}_0} H_*(I^{\bar{p}}C_\bullet^T(X)) = \varinjlim_{T \in \mathcal{T}_0} I^{\bar{p}}H_*^T(X)$, where $I^{\bar{p}}H_*^T(X) = I^{\bar{p}}H_*(|K|)$ for $T = (K, k)$.

Definition 8.27. Let L be a subcomplex of K. L is called a full subcomplex if

$$\forall \sigma \in K \text{ with vertices in } L, \text{ then } \sigma \in L$$

Definition 8.28. An admisissible triangulation T of PL filtered space X with filtration $\{X^i\}$ is called full triangulation if all X^i is a full subcomplex of X.

Theorem 8.29. Let X be a PL filtered space, T a full triangulation of X, and T' any subdivision of T. Then

$$I^{\bar{p}}C_*^T(X) \longrightarrow I^{\bar{p}}C_*^{T'}(X)$$

is an isomorphism.

Corollary 8.30.

$$I^{\bar{p}}\mathcal{H}_*(X) = \varinjlim_{T' \in \mathcal{T}_0} H_*(I^{\bar{p}}C_\bullet^{T'}(X)) = H_*\left(\varinjlim_{T' \in \mathcal{T}_0} I^{\bar{p}}C_\bullet^T(X)\right) = H_*(I^{\bar{p}}C_\bullet^T(X)) = I^{\bar{p}}H_*^T(X).$$

8.2 Computate $\mathbb{R}^2$ with two degeneracy lines

In this section, we compute the example in Fig 23. It is $\mathbb{R}^2$ with two degeneracy lines L_1 and L_2.

We have filtration $X_2 \supseteq X_1 \supseteq X_0 \supseteq X_{-1}$ where $X_2 = \mathbb{R}^2$, $X_1 = L_1 \cup L_2$, $X_0 = L_1 \cap L_2$.

The strata are shown in Fig24

We only need to choose a full triangulation to compute PL intersection homology. We pick triangulation in Fig25.

The methodology to compute is classifying i-simplexes into several types, see Fig26

We assume perversity are same on O_1, O_2, O_3, O_4:

$$\bar{p} : \{\text{Strata of X}\} \to \mathbb{Z}$$

$$R_i \mapsto 0, i = 1, 2, 3, 4$$

$$O_i \mapsto \bar{p}(1), i = 1, 2, 3, 4$$

$$T \mapsto \bar{p}(2)$$

Remark 8.31. The assumption $\bar{p}(O_1) = \bar{p}(O_2) = \bar{p}(O_3) = \bar{p}(O_4)$ for simplicity. We shall throw this assumption after we compute this simple case.

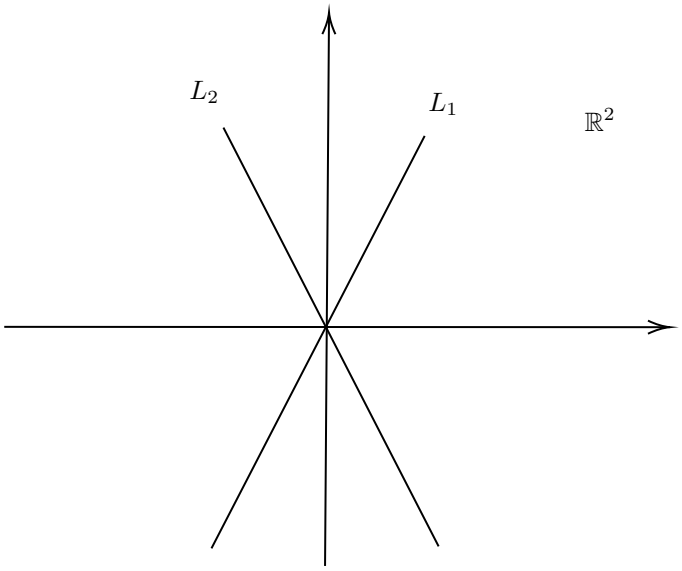

Figure 23: $\mathbb{R}^2$ with two degeneracy lines L_1 and L_2

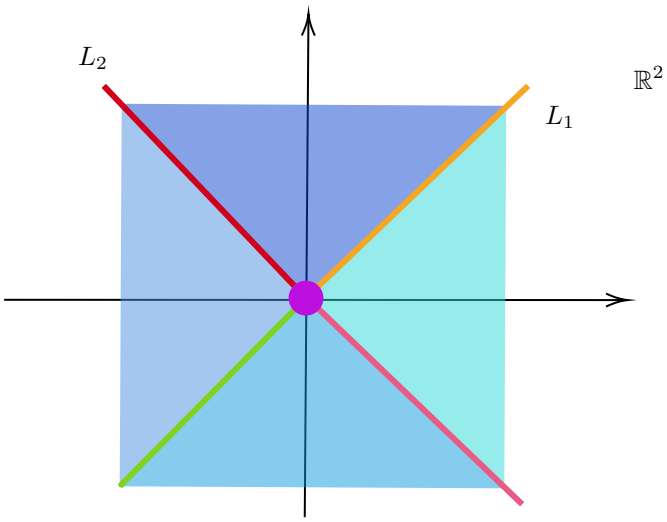

Figure 24: Stratums:There are four strata in $X_2 - X_1$, depicted in blue; There are four strata in $X_1 - X_0$, depicted in red, pink, yellow and green; There is one stratum in X_0, depicted in purple

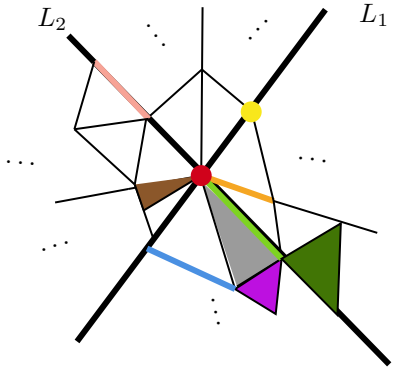

Figure 25: A full triangulation

0-simplex:	type I_0	Intersects with X_0
	type II_0	Intersects with $X_1 - X_0$
1-simplex:	type I_1	Only intersects with $X_1 - X_0$ of dim 1
	type II_1	Only intersects with $X_1 - X_0$ of dim 0
	typeIII_1	Intersects with $X_1 - X_0$, X_0
	typeIV_1	Only intersects with X_0
2-simplex:	type I_2	Intersects with $X_1 - X_0$, X_0
	type II_2	Only intersects with $X_1 - X_0$ of dim 1
	type III_2	Only intersects with $X_1 - X_0$ of dim 0
	type IV_2	Only intersects with X_0

Figure 26: Types of simplexes: we ignore the intersection with $X_2 - X_1$ since we can always ignore the allowability condition on regular strata. The sub-index of a type denotes the dimension of the simplex, and the corresponding examples are depicted in the same color in Fig25

The following steps compute the allowability condition for simplexes of dimension 0, 1, 2.

- Let η be any 2-simplex. It is allowable if
  - $dim(\eta \cap X_0) \leqslant 2 - 2 + \bar{p}(2) = \bar{p}(2)$
  - $dim(\eta \cap (X_1 - X_0)) \leqslant 2 - 1 + \bar{p}(1) = \bar{p}(1) + 1$
- Let e be any 1-simplex. It is allowable if
  - $dim(e \cap X_0) \leqslant 1 - 2 + \bar{p}(2) = \bar{p}(2) - 1$
  - $dim(e \cap (X_1 - X_0)) \leqslant 1 - 1 + \bar{p}(1) = \bar{p}(1)$
- Let v be any 0-simplex. It is allowable if
  - $dim(v \cap X_0) \leqslant -2 + \bar{p}(2)$
  - $dim(v \cap (X_1 - X_0) \leqslant -1 + \bar{p}(1))$

These allowability conditions suggest that we need to discuss the problem in 16 cases based on the value ranges of $\bar{p}(1)$ and $\bar{p}(2)$. In each of the 16 cases, we have labeled the allowable simplices for that case; see Fig27.

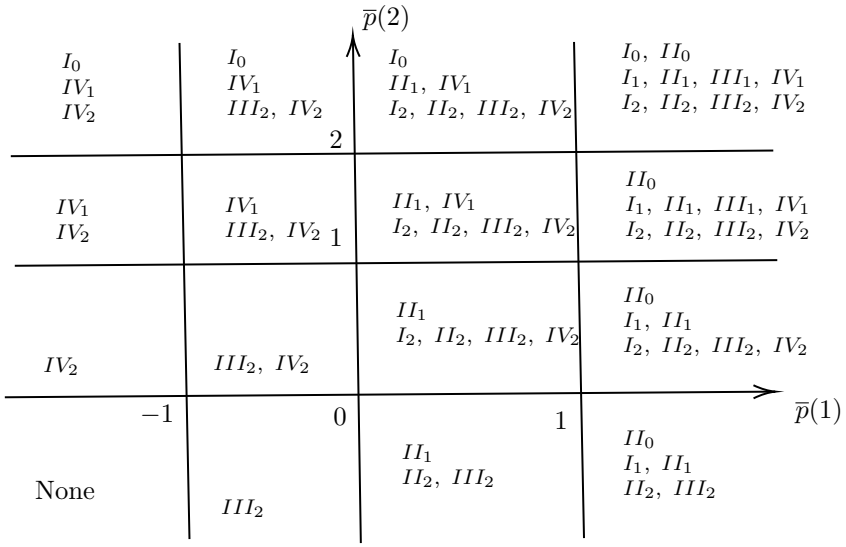

Figure 27: The allowable simplex type in each case. Note that all cases contain points on the line. e.g., the bottom right box is $\bar{p}(2) < 0$, $\bar{p}(1) \geqslant 1$.

Remark 8.32. Fig27 is obtained by combining three figures in Fig28.

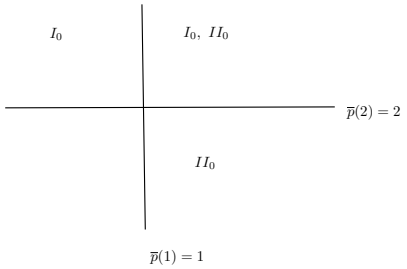

(a) Analysis for 0-simplex

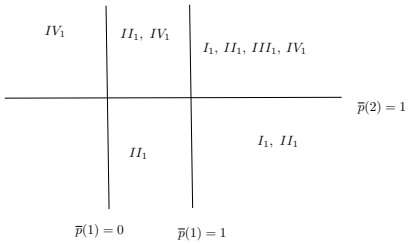

(b) Analysis for 1-simplex

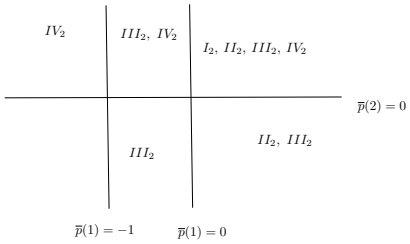

(c) Analysis for 2-simplex

Figure 28: Allowable simplexes

Example 8.33. Consider the case $1 \geqslant \bar{p}(2) < 2$, $\bar{p}(1) < -1$. In this case, we can see in Fig27 that types IV_1 and IV_2 are allowable. With IV_1, any allowable 0-simplex can be homologous to each other, so $I^{\bar{p}}H_0 = \mathbb{Z}$. The allowable 1-cycles lie in regular strata, so all 1-cycles are trivial, thus $I^{\bar{p}}H_1 = 0$. There is no 2-cycle, so $I^{\bar{p}}H_2 = 0$.

The other cases are obtained similarly.

The computation results are shown in Fig29.

Example 8.34. We provide some example loops, see Fig30. For $\bar{p}(1) < 0$, $\bar{p}(2) \geqslant 1$, the loops in (a) are trivial, i.e., they are bounded by allowable 2-chains.

For $\bar{p}(1) < 0$, $\bar{p}(2) < 1$, the only allowable loops in (b) are trivial loops in regular stratum.

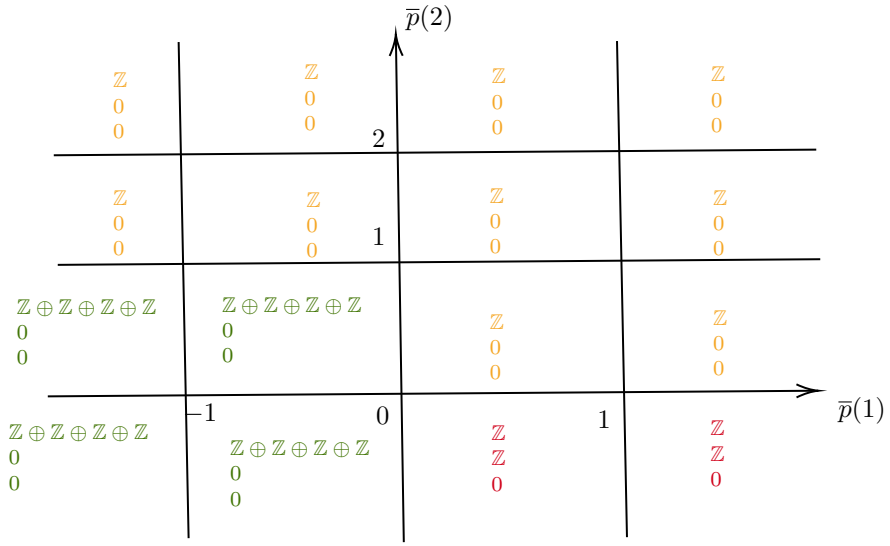

Figure 29: Intersection homology of $\mathbb{R}^2$ with two singular lines:from top to bottom is $I^{\bar{p}}H_0$, $I^{\bar{p}}H_1$, $I^{\bar{p}}H_2$

Consider the case $\bar{p}(1) \geqslant 1$, $\bar{p}(2) \leqslant 0$ in (c), the loop 1, 2, 3 are trivial and loop 4 is nontrivial, generated $I^{\bar{p}}H_1 = \mathbb{Z}$.

Analysis the results:

- In Fig29, from yellow region to green region, we "see" the two singular lines; From yellow region to red region, we "see" the singular point at the origin.
- It's equal to regular homology $H_*(\mathbb{R}^2)$ for nonnegative perversity. More discussion can be seen in Conjecture 3.4.
- We divide the results in Fig29 into four parts:A, B, C, D, see Fig31.

  In part A, type IV_1 are allowable so $I^{\bar{p}}H_0 = \mathbb{Z}$. The only allowable 1-simplex is IV_1, so any 1-cycle lies in regular strata or touches X_0. Hence $I^{\bar{p}}H_1 = 0$.

  In part B, all 2-simplex are allowable, so $I^{\bar{p}}H_1 = 0$. Since type II_1 is allowable in any case, so $I^{\bar{p}}H_0 = \mathbb{Z}$.

  In part C, four types of 1-simplexes are not allowable, so there are four path components, and thus $I^{\bar{p}}H_0 = \mathbb{Z}\oplus\mathbb{Z}\oplus\mathbb{Z}\oplus\mathbb{Z}$. All allowable 1-cycle lie in regular stratum, so $I^{\bar{p}}H_1 = 0$.

  In part D, the type II_1 is allowed, so $I^{\bar{p}}H_0 = \mathbb{Z}$. There is a nontrivial 1-cycle that is the one encloses the origin.

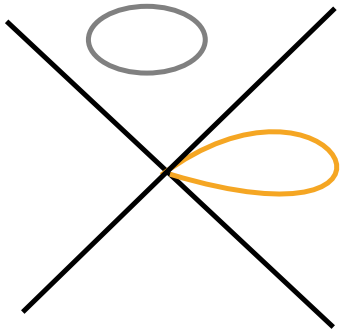

(a) $\bar{p}(1) < 0$, $\bar{p}(2) \geqslant 1$

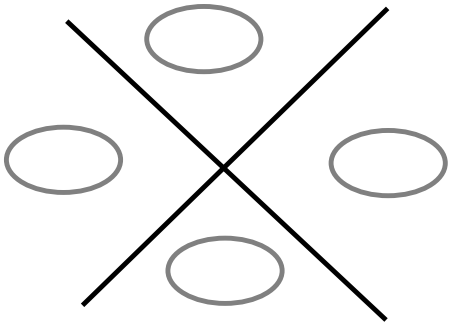

(b) $\bar{p}(1) < 0$, $\bar{p}(2) < 1$

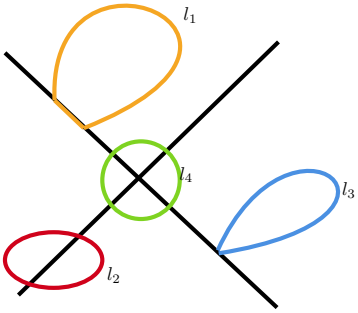

(c) $\bar{p}(1) \geqslant 1$, $\bar{p}(2) \leqslant 0$

Figure 30: Example loops

Conjecture 8.35. With nonnegative perversity, the intersection homology of smooth 2-manifold is the same as the general homology.

Proof. (Not strict)

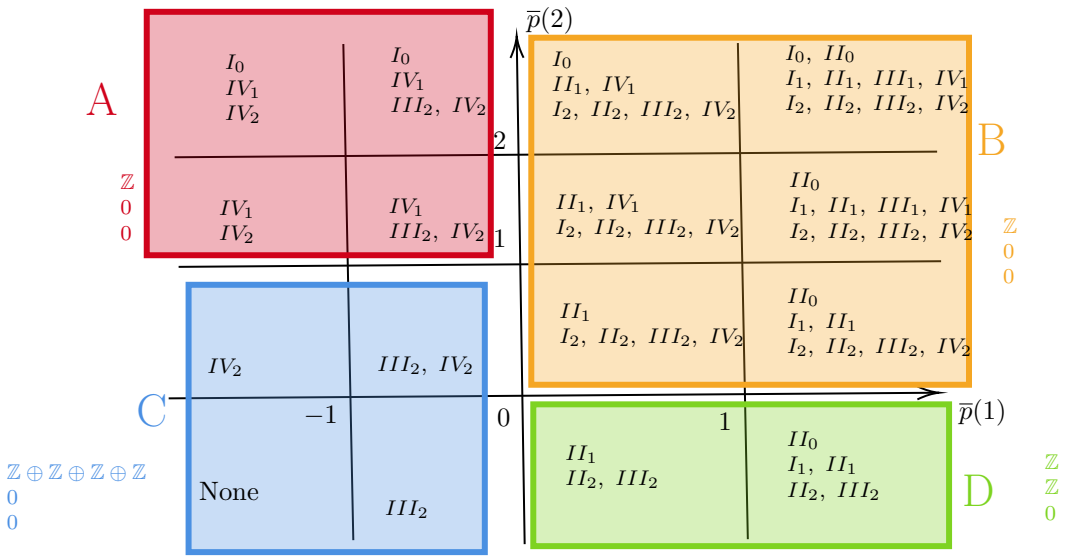

Figure 31: We divide the results into A, B, C, D four parts

- Let η be any 2-simplex. It's allowable if
  - $dim(\eta \cap X_0) \leqslant 2 - 2 + \bar{p}(2) = \bar{p}(2)$
  - $dim(\eta \cap (X_1 - X_0)) \leqslant 2 - 1 = \bar{p}(1) = \bar{p}(1) + 1$

  When perversity is nonnegative, all 2-simplexes are allowable up to homologous, i.e., $C_2^{\bar{p}}(X) = C_2(X)$ up to homologous.

- Let e be any 1-simplex. It is allowable if
  - $dim(e \cap X_0) \leqslant 1 - 2 + \bar{p}(2) = \bar{p}(2) - 1$
  - $dim(e \cap (X_1 - X_0)) \leqslant 1 - 1 + \bar{p}(1) = \bar{p}(1)$

  From the condition, we find that all 1-simples intersect with $X_1 - X_0$ of 0-dimension, and uncontaining X_0 is allowable. Since all 2-simplexes are allowable and it is a smooth manifold, we can always (I guess) homologous a 1-simplex to intersect with $X_1 - X_0$ of 0-dimension and do not contain X_0. Hence all 1-simplex is allowable up to homologous, i.e., $C_1^{\bar{p}}(X) = C_1(X)$ up to homologous.

- Let v be any 0-simplex. It is allowable if
  - $dim(v \cap X_0) \leqslant -2 + \bar{p}(2)$
  - $dim(v \cap (X_1 - X_0) \leqslant -1 + \bar{p}(1))$

We find that all 0-simplex not intersecting X_1 is allowable from the condition. Since all 1-simplexes are allowable and we are in a smooth manifold, we can always (I guess) homologous a 0-simplex to a 0-simplex not intersect X_1. So, all 0-simplex is allowable up to homologous, $C_0^{\bar{p}}(X) = C_0(X)$ up to homologous.

Hence, $I^{\bar{p}}H_*(X) = H_*(X)$.

□

Compute for the perversity that is different in the strata, the interesting result is that when $\bar{p}(2) < 0$, $\bar{p}(O_1) = \bar{p}(O_2) \geqslant 1$ and $\bar{p}(O_3) = \bar{p}(O_4) < 0$, we have $I^{\bar{p}}H_0(X) = \mathbb{Z} \oplus \mathbb{Z}$, $I^{\bar{p}}H_1(X) = 0$, $I^{\bar{p}}H_0(X) = 0$, which means that we only see one of the two singular lines. Other cases are the same and not very interesting. The non-GM case is computed the same as the GM case but still needs to be rechecked.

8.3 Compute $\mathbb{R}^2$ with one singulr point

The parametrization space of 2-band Hermitian system is $\mathbb{R}^2$ with a single singular at origin, see Fig32.

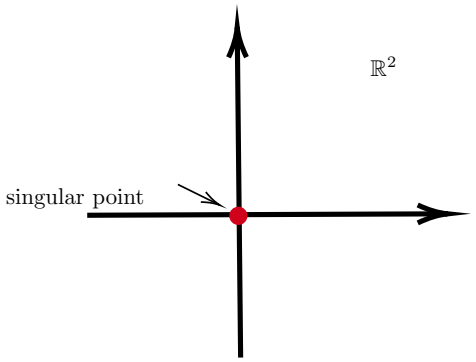

Figure 32: $\mathbb{R}^2$ with a singular point

The types of simpleces are in Fig33 and the allowable simplex in each case are in Fig34.

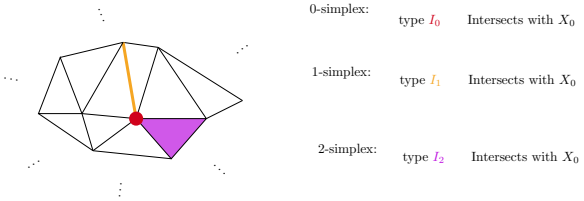

Figure 33: Types of simpleces

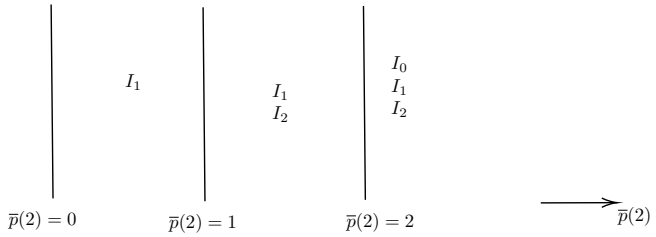

Figure 34: Allowable simplex in each case

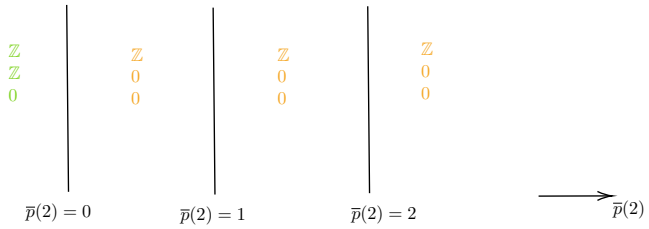

Figure 35: Intersection homology of $\mathbb{R}^2$ with one singular point:from top to bottom is $I^{\bar{p}}H_0$, $I^{\bar{p}}H_1$, $I^{\bar{p}}H_2$

By similar calculation, the results are in Fig35.

Analysis: From yellow region to green region, the $I^{\bar{p}}H_1(\mathbb{R})$ varies from 0 to $\mathbb{Z}$, meaning that we detect the singular point at the origin.

8.4 Intersection homology of swallowtail

We consider the filtered space $\mathbb{R}^3$ with filtration $X_3 \supset X_2 \supset X_1 \supset X_0 \supset X_{-1} = \emptyset$ where $X_3 = \mathbb{R}^3$, X_2 is the yellow surface, X_1 is the red and purple intersection lines and X_0 is the origin point, see Fig36.

Since there is no nontrivial 3-cycle in $C_3(\mathbb{R}^3)$, so is $I^{\bar{p}}C_3(\mathbb{R}^3)$. Thus $I^{\bar{p}}H_3(\mathbb{R}^3) = 0$.

Degree 0 intersection homology

Type of 0-simplex and 1-simplex is shown in Fig37.

The allowable 1 and 0-simplex for different perversity is shown in Fig38.

How to obtain Figure38: Here we take type III_1 for example. Similar argument in Section?, the allowable 1-simplex e satisfies the inequality

$$\begin{cases} dim(e \cap X_0) \leqslant \bar{p}(3) - 2 \\ dim(e \cap (X_1 - X_0)) \leqslant \bar{p}(2) - 1 \\ dim(e \cap (X_2 - X_1)) \leqslant \bar{p}(1) \end{cases}$$

We check Fig37 that the type III_1 intersects X_0 at 0 and intersects $X_1 - X_0$ at dimension 1. Taking the left hand side be 0 and 1 in the first and second equation, respectively, we have the type III_1 is allowable when $0 \leqslant \bar{p}(3) - 2$ and

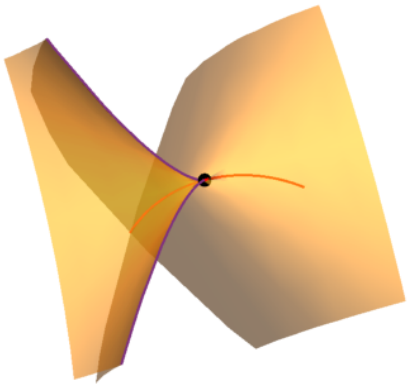

Figure 36: Filtration of swallowtail

0-simplex:	type I_0	Only interseccts with X_0
	type II_0	Only intersects with $X_1 - X_0$
	type III_0	Only intersects with $X_2 - X_1$
1-simplex:	type I_1	Only intersects with $X_1 - X_0$ at dim 1
	type II_1	Only intersects with $X_2 - X_1$ at dim 1
	type III_1	Intersects with X_0 at dim 0 and with $X_1 - X_0$ at dim 1
	type IV_1	Intersects with $X_3 - X_2$ at dim 1 and with $X_1 - X_0$ at dim 0
	type V	Intersects with $X_2 - X_1$ at dim 1 and with $X_1 - X_0$ at dim 0
	type VI_1	Intersects with X_0 at dim 0 and with $X_2 - X_1$ at dim 1
	type VII_1	Intersects with $X_3 - X_2$ at dim 1 and with $X_2 - X_1$ at dim 0
	type $VIII_1$	Intersects with X_0 at dim 0 and with $X_3 - X_2$ at dim 1

Figure 37: Types of simplices

$1 \leqslant \bar{p}(2) - 1$, i.e., $\bar{p}(3) \geqslant 2$ and $\bar{p}(2) \geqslant 2$, which is shown in Fig38. Also note that we omit the intersection at $X_3 - X_2$ since it's a regular stratum.

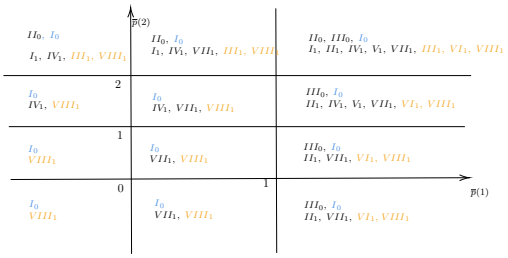

Figure 38: Classes of perversity. The yellow types are allowable when $\bar{p}(3) \geqslant 2$ and the blue ones are allowable when $\bar{p}(3) \geqslant 3$.

Sketch of computation: To illustrate more explicitly, we divide the $\bar{p}(1)\bar{p}(2)\bar{p}(3)$-space into three regions. In the region A, the type IV_1 simplexes are allowable, which means we can have path across singular lines X_1 to connect three connected components of $X_3 - X_2$; In the region B, the type VII_1 simplexes are allowable, which means we can have path across singular surface $X_2 - X_1$ to connect three connected components of $X_3 - X_2$; In the region C with $\bar{p}(3) \geqslant 2$, the type $VIII_1$ simplexes are allowable, which means we can have path across X_0 to connects the three connected components of $X_3 - X_2$; In the region C with $\bar{p}(3) < 2$, no simplexes hitting singular part X_2 are allowable, hence we could see the three connected components of $X_3 - X_2$.

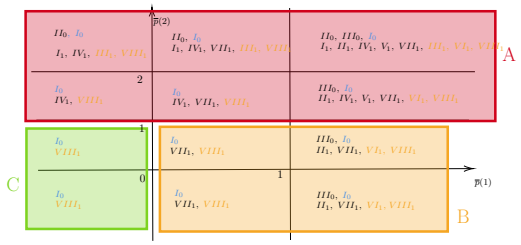

Figure 39: We divided the $\bar{p}(1)\bar{p}(2)\bar{p}(3)$-space into 3 parts

The degree 0 intersection homology is shown in Fig40, which can be formulated as:

the degree-0 intersection homology=

$$\begin{cases} \mathbb{Z} \oplus \mathbb{Z} \oplus \mathbb{Z} & \text{if } \bar{p}(1) < 0,\ \bar{p}(2) < 1,\ \text{and } \bar{p}(3) < 2 \\ \mathbb{Z} & \text{otherwise} \end{cases}$$

Analysis: 0-degree intersection homology depict connected components. By regulating the three parameters, the degree 0 intersection group changes from $\mathbb{Z}$ to $\mathbb{Z} \oplus \mathbb{Z} \oplus \mathbb{Z}$, during which we detect the three regions Reg I, II, III, which

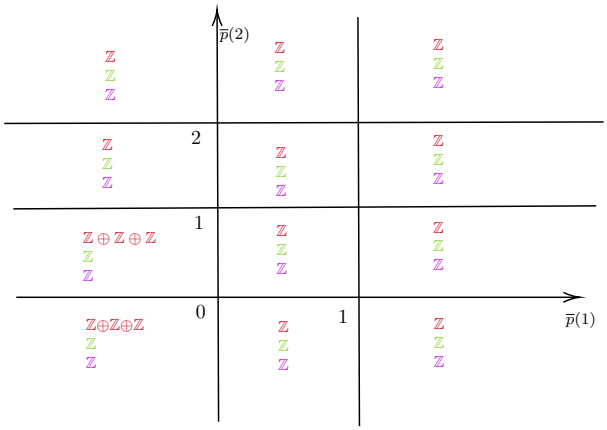

Figure 40: The red is for $\bar{p}(3) < 2$; the green is for $2 \leqslant \bar{p}(3) < 3$; the purple is for $\bar{p}(3) \geqslant 3$

are the three connected components of the complementary space of swallowtail in $\mathbb{R}^3$, see Fig36.

Degree 1 **intersection homology**

Type of 2-simplex is as following:

Table 2: Types of simplices

type I_2	Only intersects with $X_2 - X_1$ at dim 2
type II_2	Intersects with $X_3 - X_2$ at dim 2 and with X_0 at dim 0
type III_2	Intersects with $X_2 - X_1$ at dim 2 and with X_0 at dim 0
type IV_2	Intersects with $X_3 - X_2$ at dim 2 and with $X_1 - X_0$ at dim 1
type V_2	Intersects with $X_3 - X_2$ at dim 2 and with $X_1 - X_0$ at dim 0
type VI_2	Intersects with $X_2 - X_1$ at dim 2 and with $X_1 - X_0$ at dim 1
type VII_2	Intersects with $X_2 - X_1$ at dim 2 and with $X_1 - X_0$ at dim 0
type $VIII_2$	Intersects with $X_3 - X_2$ at dim 2 and with $X_2 - X_1$ at dim 1
type IX_2	Intersects with $X_3 - X_2$ at dim 2 and with $X_2 - X_1$ at dim 0
type X_2	Intersects with $X_2 - X_1$ at dim 2, with $X_1 - X_0$ at dim 1, and with X_0 at dim 0
type XI_2	Intersects with $X_3 - X_2$ at dim 2, with $X_2 - X_1$ at dim 1, and with X_0 at dim 0
type XII_2	Intersects with $X_3 - X_2$ at dim 2, with $X_1 - X_0$ at dim 1, and with X_0 at dim 0
type $XIII_2$	Intersects with $X_3 - X_2$ at dim 2, with $X_2 - X_1$ at dim 1, and with $X_1 - X_0$ at dim 0

The allowable 2 and 1-simplex for different perversity is shown in Fig41.

Sketch of computation: Some important loops potentially could be generators of intersection homology groups; see Fig42. Besides those loops, we also need to consider some loops that hit (not enclose) the singular spaces $X_2 - X_1$, $X_1 - X_0$, or X_0.

To illustrte more explicitly, we divide the $\bar{p}(1)\bar{p}(2)\bar{p}(3)$-space into five regions, see Fig43.

Figure 41: Classes of perversity. The blue is allowable when $\bar{p}(3) \geqslant 1$ and the yellow is allowable when $\bar{p}(3) \geqslant 2$

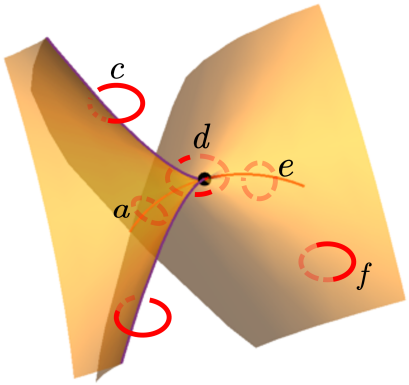

Figure 42: Some important loops

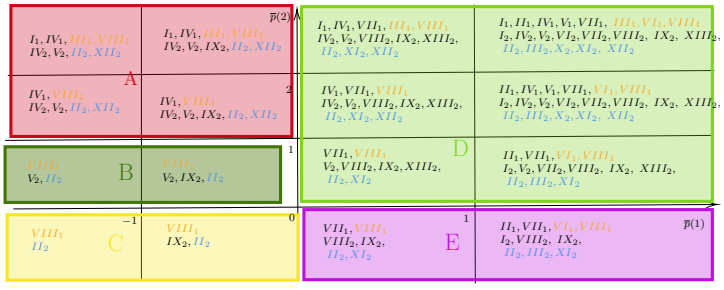

Figure 43: We divided the $\bar{p}(1)\bar{p}(2)\bar{p}(3)$-space into five parts

In the region A, the allowable 1-cycle cannot transverse the singular surface at $X_2 - X_1$ but can hit X_1. Since the type V_2 and IV_2, the 1-cycle e is bounded. Hence, the intersection homology here is all zero.

In the region B, no 1-cycles could hit X_2. However, the type V_2 is allowable, so the 1-cycle e is trivial. Hence, the intersection homology here is all zero.

In the region C, no 1-cycles are allowed to transverse X_2. The 1-cycle e is allowed, but the type V_2 is not allowable, making e a generator of intersection homology. Hence, the intersection homology here is all $\mathbb{Z}$.

In the region D, 1-cycles are allowed to transverse the singular surface X_2. The type V_2, $VIII_2$, IX_2, $XIII_2$ are allowed, and the 1-cycles a, b, c, d, e, f are all bounded, so the intersection homology here are all zero.

In the region E with $\bar{p}(3) < 1$, the three 1-cycles a, b, c are all allowed and they are none trivial. Since type $VIII_2$ and IX_2 are allowed, $e = d = a + b + c$ which is also nontrivial. In the region E with $\bar{p}(3) \geqslant 1$, the type II_2 and XI_2 are allowable, making d (also e) being bounded. Hence the intersection here is $\mathbb{Z} \oplus \mathbb{Z} \oplus \mathbb{Z}/(a + b + c = 0)$

The degree 1 intersection homology is shown in Fig44, which can be formulated as

The degree-1 intersection homology=

$$\begin{cases} \mathbb{Z}e & \text{if } \bar{p}(1) < 0,\ \bar{p}(2) < 0,\ \text{and } \forall \bar{p}(3) \in \mathbb{Z} \\ \mathbb{Z}a \oplus \mathbb{Z}b \oplus \mathbb{Z}c & \text{if } \bar{p}(1) \geqslant 0,\ \bar{p}(2) < 0,\ \text{and } \bar{p}(3) < 1 \\ \mathbb{Z}a \oplus \mathbb{Z}b \oplus \mathbb{Z}c/(a + b + c = 0) & \text{if } \bar{p}(1) \geqslant 0,\ \bar{p}(2) < 0,\ \text{and } \bar{p}(3) \geqslant 1 \\ 0 & \text{otherwise} \end{cases}$$

where the generators a, b, and c are shown in Fig**??**.

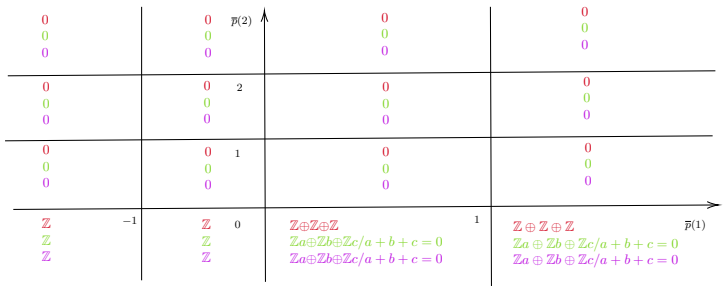

Figure 44: The red is for $\bar{p}(3) < 1$; the green is for $1 \leqslant \bar{p}(3) < 2$; the purple is for $\bar{p}(3) \geqslant 2$

Analysis:

- Loops in Fig**??** are satisfying $a + b + c = d$, $d = e$ in intersection groups containing a, b, c, d, e. These equations mean the three singular lines can fuse to the isolated singular lines.

- The group $\mathbb{Z}e$ detects the isolated singular line in the swallowtail but does not detect the three singular lines on the surface.
- The group $\mathbb{Z}a \oplus \mathbb{Z}b \oplus \mathbb{Z}c/(a+b+c=0)$ detects three singular lines on the surface but does not detect the isolated singular line since loop $e = d = 0$.
- The group $\mathbb{Z}a \oplus \mathbb{Z}b \oplus \mathbb{Z}c$ detects both the three singular lines on the surface and the isolated singular line since loop $e = d = a + b + c \neq 0$.

  All of the above shows that the isolated singular line strongly relates to the three singular lines on the surface.

Degree 2 intersection homology

The intersection cases of 3-simplex can be classified by intersection dimension. The equivalence condition for those 3-simpleces being alllowable is shown in Fig45.

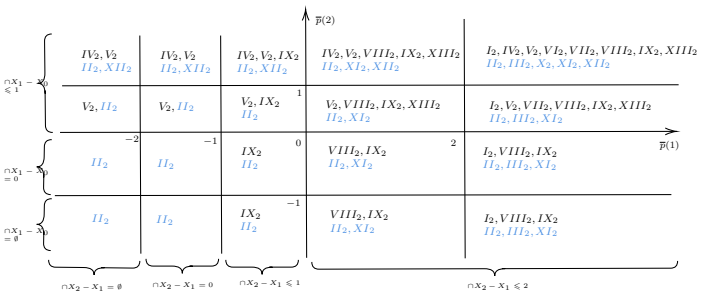

Figure 45: Allowable 2 and 3-simpleces for different perversity conditions; The blue ones are allowable when $\bar{p}(3) \geqslant 1$; The allowable 3-simplex with different intersection dimension condition are shown in the picture, e.g., the 3-simplex that does not intersect $X_2 - X_1$ is for $\bar{p}(1) < -2$; Note that the condition corresponds to whether 3-simplex could intersect the X_0 is not denoted in the picture. The 3-simplex intersect with X_0 is allowed only when $\bar{p}(3) \geqslant 0$

Sketch of computation: The possible nontrivial 2-cycles are the ones enclosing the origin, which need the type of 2-simplexes that intersect with $X_1 - X_0$ at $\geqslant 0$ -dimension and $X_2 - X_1$ at $\geqslant 1$-dimension.

Therefore, for $\bar{p}(3) \geqslant 0$, the 3-simplex intersecting X_0 is allowed, so the intersection homology for $\bar{p}(3) \geqslant 0$ are all trivial, i.e., the green and purple one in Fig47 are all zero.

To illustrte more explicitly, we divide the $\bar{p}(1)\bar{p}(2)\bar{p}(3)$-space into three regions, see Fig46.

In the region A with $\bar{p}(3) < 0$, type V_2, $VIII_2$, IX_2 are allowable, so the 2-cycle enclose the origin are allowed. However, the 3-simplex cannot intersect the origin, making this 2-cycle bounded. Hence, the intersection group is $\mathbb{Z}$.

In the region B, no allowable 2-cycles can transverse the singular surface X_2; thus, no 2-cycles can enclose the origin. Hence, the intersection homology here is zero.

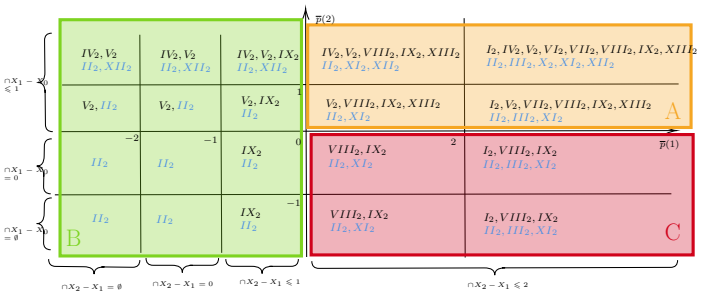

Figure 46: We divided the $\bar{p}(1)\bar{p}(2)\bar{p}(3)$-space into three parts

In the region C, no allowable 2-cycles can hit singular line $X_1 - X_0$, so no 2-cycles can enclose the origin. Hence, the intersection homology here is zero.

The degree 2 intersection homology is shown in Fig47, which can be formulated as

The degree-2 intersection homology=

$$\begin{cases} \mathbb{Z} & \text{if } \bar{p}(1) \geqslant 0,\ \bar{p}(2) \geqslant 0,\ \text{and } \bar{p}(3) < 0 \\ 0 & \text{otherwise} \end{cases}$$

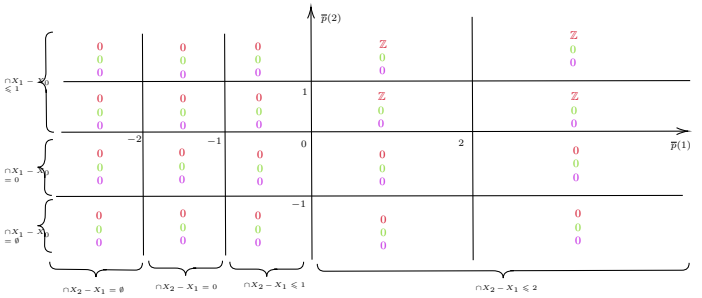

Figure 47: The red is for $\bar{p}(3) < 0$; the green is for $0 \leqslant \bar{p}(3) < 1$; the purple is for $\bar{p}(3) \geqslant 1$

Analysis: The $\mathbb{Z}$ group is generated by a sphere enclosing the origin. Hence, during the degree 2 intersection group changing from 0 to $\mathbb{Z}$ by tuning parameters, we detect the singular point MP (meeting point) at the origin.

8.5 An interesting phenomenon

By the results of intersection homology of $\mathbb{R}^2$ with a singular point at the origin, $\mathbb{R}^2$ with two singular lines, and swallowtail in $\mathbb{R}^3$, we find the following interesting phenomenon: It seems that the degree n intersection homology could only detect the $3-(n+1)$ dimension singularities.

Firstly, we need to describe "detect" more explicitly. It is clear that if an n-chain enclose (not intersect with it) a r dimension singularity and no $n+1$-chain with n-chain could intersect with r dimension singularity for some perversity, we detect this singularity. For example, a sphere encloses the origin in the swallowtail example. These are all the cases in the above computations.

Since an n-chain encloses an r dimension singularity, which means $r = 3 - (n+1)$, it seems we describe the phenomenon.

However, are there any other cases? For example, in Fig48, the yellow surface is a singular surface, and the black 1-chain a intersects with these singular surfaces. If there is no allowable 2-chain with 1-chain a being a boundary, then this 1-chain is nontrivial and can detect the singular surface.

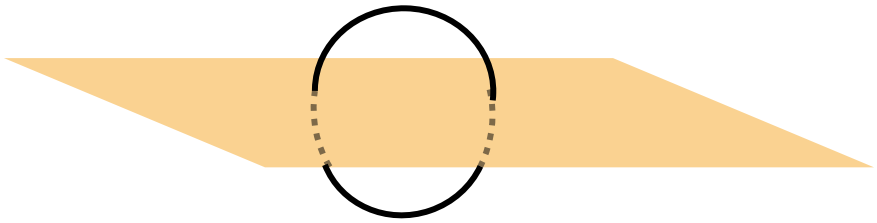

Figure 48: A possible nontrivial chain that not be the enclose type

But it's impossible, by the following property.

Property 8.36. For an allowable n-chain γ, if it intersects with a singular stratum S_i, where S_i has codimension i, and there exists $(n+1)$-chain η with $\partial\eta = \gamma$ and $dim(\gamma \cap S_i) \geqslant dim(\eta \cap S_i) - 1$, then γ is trivial.

Proof. Consider an allowable n-chain γ and $(n+1)$-chain η in $C_{n+1}(\mathbb{R}^3)$ with $\partial\eta = \gamma$. η may not be allowable, but we want to show η is allowable, i.e., $dim(\eta_j \cap S_i) \leqslant n + 1 - i + \bar{p}(i)$ for each $(n+1)$-simplex η_j. Clearly, as a subspace, $dim(\eta_j \cap S_i) \leqslant dim(\eta \cap S_i)$ for each j. Consider the $(n+1)$-simplex η_{j_0} with $dim(\eta_{j_0} \cap S_i) = dim(\eta \cap S_i)$. If η_{j_0} is allowable, then $dim(\eta_j \cap S_i) \leqslant dim(\eta \cap S_i) = dim(\eta_{j_0} \cap S_i) \leqslant n + 1 - i + \bar{p}(i)$ for each j, complete the proof.

Since γ is allowable, so for each n-simplex γ_k in γ, we have $dim(\gamma_k \cap S_i) \leqslant n - i + \bar{p}(i)$. As a subspace, we also have $dim(\gamma_k \cap S_i) \leqslant dim(\gamma \cap S_i)$ for each k. Let γ_{k_0} be the n-simplex in γ with $dim(\gamma_{k_0} \cap S_i) = dim(\gamma \cap S_i)$. Hence, we have $dim(\gamma \cap S_i) = dim(\gamma_{k_0} \cap S_i) \leqslant n - i + \bar{p}(i)$. Then we obtain that $\bar{p}(i) \geqslant dim(\gamma \cap S_i) - n + i$. Since $dim(\gamma \cap S_i) \geqslant dim(\eta \cap S_i) - 1$, $\bar{p}(i) \geqslant dim(\eta \cap S_i) - n - 1 + i = dim(\eta_{j_0} \cap S_i) - n - 1 + i$, meaning that η_{j_0} is allowable.

Hence γ is bounded by η in the intersction homology and thus γ is trivial. □

Example 8.37. The 1-chain γ in Fig48 must be trivial, since $dim(\gamma \cap S_i) = 0 \geqslant dim(\eta \cap S_i) = 1 - 1 = 0$

Remark 8.38. The condition $dim(\gamma \cap S_i) \geqslant dim(\eta \cap S_i) - 1$ holds for the most cases. Otherwise, $dim(\gamma \cap S_i) \leqslant dim(\eta \cap S_i) - 2$, which is ridiculous since $dim(\eta) = dim(\gamma) + 1$.

Note that we discuss the cases where γ intersects with only one strata. It can also be generalized to the case where γ intersects with finitely many strata.

Corollary 8.39. Let Γ be an allowable n-chain intersecting with $\{S_i^1, \cdots, S^{n_i} | i \in I, n_i \in \mathbb{N}\}$. If there exists an $(n+1)$-chain η with $\partial\eta = \gamma$ and $dim(\gamma \cap S_i^l) \leqslant dim(\eta \cap S_i^l) - 1$ for all $i \in I$ and $1 \leqslant j \leqslant n_i$, then γ is trivial.

Therefore, to have the nonsingular generator of intersection homology, we need the n-chain **NOT** intersects with strata, which means enclosing the singularities.

8.6 Further work: Intersection homotopy of the parameter space

Beside intersection homology, we also need intersection homotopy of the parameter space.

By analogy with intersection homology, Gajer defined intersection homotopy in [6] as follows:

Definition 8.40. Let (X, Ψ) be a space with filtration $\Psi : X^n \supseteq X^{n-1} \supseteq \cdots X^1 \supseteq X^0 \supseteq X^{-1} = \emptyset$.

- Let P be a polyhedron (topological space with admissible triangulations) of dimension k. A continuous map $f : P \to X$ is $\bar{p}$-allowable with Ψ if $f^{-1}(X^s)$ is contained in a sub polyhedron of P whose dimension less or equal than $k - s + \bar{p}(s)$, written as $f^{-1}(X^s) \leqslant k - s + \bar{p}(s)$.
- Let M be a PL manifold (manifold with admissible triangulations) of dimension k. A continuous map $f : M \to X$ is of perversity $\bar{p}$ with respect to a filtration Ψ if f and $f|_{\partial M}$ are $\bar{p}$-allowable maps with respect to Ψ.
- Let f_0, f_1 be two maps. f_0, f_1 are called $\bar{p}$-homotopic if there is a homotopy $M \times I \to X$ between f_0 and f_1 which is of perversity $\bar{p}$.
- Let x be the base point in the top stratum $X^0 - X^1$ of X. The kth perversity $\bar{p}$ intersection homotopy group, $I_{\bar{p}}\pi_k(X, x)$, is the $\bar{p}$-homotopy classes of perversity $\bar{p}$ maps $(S_k, s) \to (X, x)$. The group structure is defined similarly to an ordinary homotopy group.

David Chataur proved the $\bar{p}$-intersection Hurewicz theorem in [2].

Theorem 8.41. Let X be a CS set and $\bar{p}$ a perversity such that $I_{\bar{p}}\pi_0(X) = 0$.

(i) For any regular point x, the p-intersection Hurewicz map

$$h_1^{\bar{p}} : I_{\bar{p}}\pi_1(X, x) \to I_{\bar{p}}\widetilde{H}_1(X; \mathbb{Z})$$

induces an isomorphism between the abelianization of $I_{\bar{p}}\pi_1(X, x)$ and $I_{\bar{p}}\widetilde{H}_1^p(X; \mathbb{Z})$.

(ii) Let $k \geq 2$. Suppose that $I_{\bar{p}}\pi_j(X) = I_{\bar{p}}\pi_j(L) = 0$ for every link L of X, and for each $j \leq k-1$. Then, the intersection Hurewicz homomorphism

$$h_j^{\bar{p}} : I_{\bar{p}}\pi_j(X, x_0) \to I_{\bar{p}}\widetilde{H}_j^p(X; \mathbb{Z})$$

is an isomorphism for $j \leq k$, and a surjection for $j = k+1$.

In [6], Gajer finds a simplicial set $\mathcal{G}_{\bar{p}}(X)$ corresponding to a finitely filtered space (X, Ψ). Gajer shows this simplicial set satisfies the Kan extension condition to define simplicial homotopy groups on $\mathcal{G}_{\bar{p}}(X)$. Then by definition we have isomorphism $I_{\bar{p}}\pi_k(X, x) \cong \pi_k(\mathcal{G}_{\bar{p}}(X), \mathcal{G}_{\bar{p}}(x))$.

Remark 8.42. This isomorphism is the intersection version of $\pi_k(X, x) \cong \pi_k(S(X), S(x))$ where $S(X)$ is the singular simplicial set of a topological space X.

Based on Gajer's work on $\mathcal{G}_{\bar{p}}(X)$, David Chataur et al. developed a method [1] to compute the intersection homotopy.
Here are the main concepts of the main theorem.

- **top perversity, dual perversity**Define the dual perversity $D\bar{p}$ as $D\bar{p}(S) := \bar{t}(S) - \bar{p}(S)$, where $\bar{t}$ is the top perversity defined by $\bar{t} := codim S - 2$.
- **(stratified homotopy link** $\text{holink}_s(X, Y)$**)** The *homotopy link* of Y in X is space

  $$\text{holink}(X, Y) = \{\omega : [0, 1] \to X | \omega(0) \in Y \text{ and } \omega(t) \in X - Y \text{ for } t \in (0, 1]\}$$

  The *stratified homotopy link* is

  $$\text{holink}_s(X, Y) = \{\omega \in \text{holink}(X, Y) | \text{for some } S_i \in \mathcal{S}_X, \omega((0, 1]) \subset S_i\}$$

  and its filtered by

  $$\text{holink}_s(X, Y)^j = \{\omega \in \text{holink}_s(X, Y) | \omega(1) \in X^j\}$$

  There are two evaluation map $\text{eval}_0 : \text{holink}(X, Y)$ and $\text{eval}_0 : \text{holink}_s(X, Y) \to Y$. The *local holink* of $x_0 \in S$, denoted by $\text{holink}_s(X, x_0)$, is the fiber at x_0 of the map $\text{eval}_0 : \text{holink}_s(X, S) \to S$.
- Let Y be a subspace of a space X. Y is said to be *forward tame* in X if there exists a neighborhood N of Y in X and a homotopy $h : N \times I \to X$ such that:
  - $h(-, 0)$ is the inclusion $N \hookrightarrow X$
  - the restriction $h(-, t) : Y \to X$ is the inclusion $Y \hookrightarrow X$ for all $t \in I$
  - $h(N, 1) = Y$
  - $h((N \setminus Y) \times [0, 1)) \subset X \setminus Y$

Let Y be a subspace of a stratified space X. Y is *stratified forward tame* in X if there exists a neighborhood N of Y in X and a homotopy $h : N \times I \to X$ satisfying:

- $h(-, 0)$ is the inclusion $N \hookrightarrow X$
- for each $t \in I$, the restriction $h(-, t) : Y \to X$ is the inclusion $Y \hookrightarrow X$
- $h(N, 1) = Y$
- $h((N \setminus Y) \times [0, 1)) \subset X \setminus Y$ is *stratum-preserving* along $[0, 1)$.

Let X be a stratified metric space. X is a *homotopically stratified space* if for any $S \subset \bar{S}'$

1. S is forward tame in $S \cup S'$,
2. the evaluation map $\text{eval}_0 : \text{holink}(S \cup S', S) \to S$ is a fibration. (Note that holink(X, Y) is not a stratified space, so here is an ordinary fibration, not a stratified fibration)

Moreover, if each stratum is a manifold without boundary and is locally closed (subset A is called locally closed in X if A is open in its closure in X) in X, then X is called a *manifold homotopically stratified space.*

Theorem 8.43. Let $(X, \bar{p})$ be a manifold homotopically stratified space with perversity $\bar{p}$ which has a finite number of strata and connected local holinks. Let Φ be the correspondence associating to any stratum $S \in \mathcal{S}$ the injection $S^{D\bar{p}(S)+1} \to D^{D\bar{p}(S)+2}$, which is the standard inclusion in **Top** of the $(D\bar{p}(S) + 1)$-sphere in the $(D\bar{p}(S) + 2)$-ball Then the linkwise localization $\mathcal{L}_\phi X$ has the homotopy type of the realization $|\mathcal{G}_{\bar{p}} X|$ of the Gajer simplicial set associated to $(X, \bar{p})$.

The perverse manifold homotopically stratified space and connected local holinks are defined in Definitions 2.1 and 2.2 in [1].

Fact 8.44. [17] $\pi_n(Y) = \pi_n(|Y|)$ for a pointed fibrant simplicial set Y after defining an appropriate group structure on $\pi_n(Y)$ for $n \geqslant 1$.

Hence, if $\mathcal{G}_{\bar{p}}(X)$ is a pointed fibrant simplicial set, then $I_{\bar{p}}\pi_n(X) = \pi_n(\mathcal{G}_{\bar{p}}(X)) = \pi_n(|\mathcal{G}_{\bar{p}}(X)|) = \pi_n(\mathcal{L}_\phi X)$.

The way to compute $\mathcal{L}_\phi X$ is as following [1]: Let $\Phi : \mathcal{S}_X \to \text{Mor}(\mathbf{Top})$ which associates to each stratum S a morphism $\Phi(S) : A_S \to B_S$ in **Top**.

Let $\mathcal{S}_X$ be the set of strata of X.

- **(f-local, f-local equivalence, and f-localization)**[7] Let $f : A \to B$ be a map in $\mathcal{T}$ between cofibrant spaces. A fibrant space W is called *f-local* if the induced map of simplicial sets $f^* : \text{Map}(B, W) \to \text{Map}(A, W)$ is a weak equivalence. A map $g : X \to Y$ between cofibrant spaces is an *f-local equivalence* if the induced map of simplicial sets $g^* : \text{Map}(Y, W) \to \text{Map}(X, W)$ is a weak equivalence for every f-local space W. An *f-localization* of a space X is an f-local space $\bar{X}$ together with an f-local

equivalence $j_X : X \to \bar{X}$. If $\mathcal{T} = \mathbf{sSet}$, let $f : A \to B$ be an injection. If $\mathcal{T} = \mathbf{Top}$, let $f : A \to B$ be an inclusion of cell complexes. By Theorem 1.3.11 in [7], there exists a natural f-localization

$$j_X : X \to L_f X$$

with j_X a cofibration for every space X.

- **(The property of $\overline{L}_f X$)** We do not know clear what $\overline{L}_f X$ is and it is defined by properties: Let $\mathcal{T}$ be one of the categories **Top** or **sSet**. There is a functorial factorization of every map $p : X \to Z$ of $\mathcal{T}$ as

$$X \xrightarrow{i} \bar{L}_f X \xrightarrow{q} Z,$$

called the *fibrewise f-localization* of p, such that the following properties are satisfied:

1. The map q is a fibration with f-local fibres and the map i is a cofibration and an f-local equivalence. Moreover, for any $z \in Z$, the map induced by i between the homotopy fibres is an f-localization.
2. For any decomposition of p as

$$X \xrightarrow{j} W \xrightarrow{r} Z,$$

where r a fibration with f-local fibres, there exists $k : \bar{L}_f X \to W$ such that $k \circ i = j$ and $r \circ k = q$. Moreover, if j is another fibrewise f-localization, then k is a weak equivalence.

- **(Construction of linkwise Φ-localization)** A recursion relation defines $\mathcal{L}_\Phi X$. The *linkwise Φ-localization* $\mathcal{L}_\Phi X$ is defined as the homotopy pushout of

$$\bar{L}_{\Phi(S)}(\mathcal{L}_\Phi \operatorname{holink}_{\mathrm{s}}(X, S)) \leftarrow \mathcal{L}_\Phi \operatorname{holink}_{\mathrm{s}}(X, S) \to \mathcal{L}_\Phi(X - S)$$

Where S is a bottom stratum of X. Since $X - S$ has one less stratum as X, so we set $\mathcal{L}_\Phi X = X$ if X has only regular strata.

References

[1] David Chataur, Martintxo Saralegi-Aranguren, and Daniel Tanré. Homotopy truncations of homotopically stratified spaces. *Proceedings of the American Mathematical Society*, 152(03):1319–1332, 2024.

[2] David Chataur, Martintxo Saralegi-Aranguren, and Daniel Tanré. Relation between intersection homology and homotopy groups. *Journal of the European Mathematical Society*, 2025.

[3] Anand Deopurkar. An introduction to intersection homology, 2010. https://deopurkar.github.io/papers/anandrd_minor_thesis.pdf.

[4] Duality142857. Rotation matrix by any axis. https://zhuanlan.zhihu.com/p/462935097?utm_psn=1821857970075607042, 2022. Accessed: 2024-08-29.

[5] Greg Friedman. *Singular Intersection Homology*. New Mathematical Monographs. Cambridge University Press, 2020.

[6] Pawel Gajer. *The intersection Dold-Thom theorem*. State University of New York at Stony Brook, 1993.

[7] Philip S Hirschhorn. *Model categories and their localizations*. Number 99. American Mathematical Soc., 2003.

[8] Jing Hu, Ruo-Yang Zhang, Yixiao Wang, Xiaoping Ouyang, Yifei Zhu, Hongwei Jia, and Che Ting Chan. Non-Hermitian swallowtail catastrophe revealing transitions among diverse topological singularities. *Nature Physics*, 19:1098–1103, 2023.

[9] Hongwei Jia, Jing Hu, Ruo-Yang Zhang, Yixin Xiao, Dongyang Wang, Mudi Wang, Shaojie Ma, Xiaoping Ouyang, Yifei Zhu, and C. T. Chan. Anomalous bulk–edge correspondence intrinsically beyond line-gap topology in non-Hermitian swallowtail gapless phase, 2024. Preprint.

[10] Hongwei Jia, Jing Hu, Ruo-Yang Zhang, Yixin Xiao, Dongyang Wang, Mudi Wang, Shaojie Ma, Xiaoping Ouyang, Yifei Zhu, and C. T. Chan. Unconventional topological edge states beyond the paradigms of line-gap topology, 2024. Preprint.

[11] Hongwei Jia, Ruo-Yang Zhang, Jing Hu, Yixin Xiao, Shuang Zhang, Yifei Zhu, and C. T. Chan. Topological classification for intersection singularities of exceptional surfaces in pseudo-Hermitian systems. *Communication Physics*, 6:293, 2023.

[12] Hongwei Jia, Ruo-Yang Zhang, Jing Hu, Yixin Xiao, Yifei Zhu, and C. T. Chan. Topological classification for intersection singularities of exceptional surfaces in pseudo-hermitian systems, 2022.

[13] N. D. Mermin. The topological theory of defects in ordered media. *Rev. Mod. Phys.*, 51:591–648, Jul 1979.

[14] Barbara Roos and Giovanni Felder. Principal bundles, hopf bundles and eigenbundles. 2022.

[15] Barbara Roos and Giovanni Felder. Principal bundles, hopf bundles and eigenbundles. 2022.

[16] Charles C. Wojcik, Xiao-Qi Sun, Tomá š Bzdušek, and Shanhui Fan. Homotopy characterization of non-hermitian hamiltonians. *Phys. Rev. B*, 101:205417, May 2020.

[17] Jie Wu. Simplicial objects and homotopy groups. In *Braids: introductory lectures on braids, configurations and their applications*, pages 31–181. World Scientific, 2010.

[18] QuanSheng Wu, Alexey A. Soluyanov, and Tomáš Bzdušek. Non-Abelian band topology in noninteracting metals. *Science*, 365:1273–1277, 2019.

[19] Chengye You. *Basics on topology*. Basics on topology, 1997.